RADC-TDR-64-174
Final Report

PLASMA KINETIC ENERGY - RF CONVERSION

TECHNICAL DOCUMENTARY REPORT NO. RADC-TDR-64-174
July 1964

Techniques Branch
Rome Air Development Center
Research and Technology Division
Air Force Systems Command
Griffiss Air Force Base, New York

Project No. 5573, Task No. 557303

(Prepared under Contract No. AF30(602)-2981 by Advanced Kinetics, Inc., 1231 Victoria Street, Costa Mesa, Calif.)

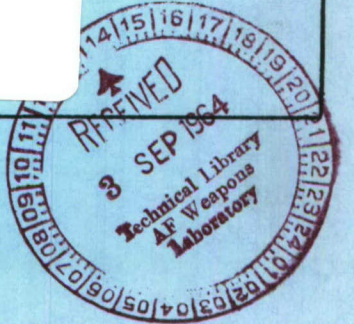

RADC-TDR-64-174
Final Report

PLASMA KINETIC ENERGY - RF CONVERSION

TECHNICAL DOCUMENTARY REPORT NO. RADC-TDR-64-174
July 1964

Techniques Branch
Rome Air Development Center
Research and Technology Division
Air Force Systems Command
Griffiss Air Force Base, New York

Project No. 5573, Task No. 557303

(Prepared under Contract No. AF30(602)-2981 by Advanced Kinetics, Inc., 1231 Victoria Street, Costa Mesa, Calif.)

FOREWORD

The following personnel have contributed to the work presented in this technical report:

Dr. R. W. Waniek

Mr. R. T. Grannan

Dr. D. G. Swanson

Mr. L. L. Wentzel

Mr. W. C. Miller

Mr. H. J. Gilsdorf

AIR FORCE, Cato Show Prtg. Co. 8/19/64 - 139 -

Key words: Plasma Oscillations; Electromagnetic Waves - Microwaves

ABSTRACT

A theoretical and experimental program is described aimed at studying the possibility of extracting microwave power from the kinetic energy of a plasma. The appropriate theoretical framework is established with the description of a radiating black body and the emission by bremsstrahlung collisions. A detailed analysis of the cyclotron radiation by a single electron and by an electron population of Maxwellian distribution is given. Problems are discussed covering the frequency distribution of the power spectrum over the harmonics and the angular distribution of the radiation. The solution of the more generalized formulation for the radiation output is indicated.

Detailed experiments were run at X-band and at K-band. The detected microwave pulse appears before onset of opacity and attains values on the order of 50 to 250 mW for a background pressure of 20 microns Hg, discharge voltages around 20 kV, and magnetic fields around 3.5 kG. The output is studied as a function of magnetic field and of the applied electric field. At K-band two peaks become apparent and these are interpreted in terms of the fundamental and the second harmonic detected in this frequency interval.

The results obtained during the experimental phase are discussed in detail. It is shown that the power output detected is too high to be explained by cyclotron radiation output from a population of temperature and density

not exceeding reasonable values. The mechanism of electron acceleration by overstability processes is introduced which would seem to explain the high radiation output as the cyclotron radiation from very high speed electrons accelerated by internal processes in the plasma.

Several pertinent tests are suggested which should be carried out in the future to explain some of the interesting features which have emerged during the course of this study.

PUBLICATION REVIEW

This report has been reviewed and is approved. For further technical information on this project, contact Mr. Frank E. Welker, EMATP, Ext. 75141.

Approved: Frank E Welker
FRANK E. WELKER
Project Engineer

Approved: Paul W. Baldwin
for Lt Col USAF
THOMAS F. BOND, JR.
Colonel, USAF
Chief, Surveillance & Control Division

FOR THE COMMANDER: Fred I Diamond
for IRVING J. GABELMAN
Chief, Advanced Studies Group

TABLE OF CONTENTS

LIST OF ILLUSTRATIONS

Evaluation

1. This program was one of two initiated to investigate the conversion of plasma kinetic energy to electromagnetic energy. There were no restrictions placed on the source of kinetic energy, however, the program was to be carried out keeping in mind the intended use of any generating techniques developed in long range radar system propagating through the atmosphere. The conversion processes were to be evaluated for very high power operation with the phase and amplitude characteristics of the radiated signal defined as a function of both power level and frequency of operation.

2. The contractor proposed cyclotron radiation from a magnetized plasma as the most feasible radiation mechanism in a plasma at the frequencies of interest. The energy source in their experiment is a high density discharge of electrons through the plasma column. A theoretical model was developed for this interaction, but initial experiments indicated that more power was being radiated than could be accounted for in a linear theory. This required a more comprehensive theoretical approach and very careful selection of parameters for evaluation in the experiment. A six month extension has been initiated with Advanced Kinetics to continue the evaluation of cyclotron radiation from a plasma and its application to device concepts usable in radar systems.

3. This program is one of several initiated to investigate non-electron tube sources of electromagnetic energy for advanced radar systems. This interaction is a bulk interaction. It takes place within the plasma itself and uses a natural resonance of the medium; hence, it doesn't require metal structures to provide the necessary resonance for gain to take place. The electron tube types used today all require metal structures with dimensions smaller than a wavelength which complicates the heat dissipation problem at higher frequencies. The magnetic field requirements over a large volume and incoherency of the output signal do, however, provide serious problems for application of this energy source to radar systems as we know them today.

Frank E. Welker

FRANK E. WELKER
Project Engineer

I) DISCUSSION OF THEORETICAL PROBLEMS

A) THE EMISSION OF ELECTROMAGNETIC WAVES FROM A HOT PLASMA

The conversion of kinetic energy of fast-moving, charged particles into electromagnetic energy is a process of basic importance and of great potential usefulness. On the cosmic scale, this conversion process is responsible for the extremely energetic bursts of radiowaves from the sun and from certain types of stars. It is known, for instance, that the radio emission from a large solar flare might amount to 10^{24} ergs[1] which is equivalent to 28,000 million kWh or 24 Megatons of TNT. Since the radiating medium is usually a high temperature plasma permeated by magnetic fields, it appears of definite interest to study the possible modes of radiation of a plasma in the laboratory with an aim at developing high peak pulse power emitters operating on principles similar to those encountered in space.

In the following, we shall present the appropriate theoretical framework for the various modes of radiation expected from a hot plasma, concentrating our analysis on the region between 1 - 100 kMc which is of particular interest in the context of this work.

1) The Emission from an Opaque Medium: Blackbody Radiation

For situations describing dense plasmas in which the radiation mean free path is much shorterthan the characteristic dimensions of the medium, the

black-body formulation may be applied[2]. After radiative equilibrium is established, each element of such a plasma radiates energy to its surroundings which, in turn, reradiate it randomly. The energy density radiated in a frequency interval df is then given by Planck's radiation law

$$W\,df = 8\pi h \frac{f^3}{c^3} \frac{1}{[\exp(hf/kT)]-1} \qquad \text{joules/m}^3 \qquad (1)$$

In regions where $hf << kT$ (and this applies quite appropriately in the microwave region where hf is about 10^{-25} joules at 1 kMc versus a typical kT of 10^{-17} joules for a 10^6 °K plasma), the Rayleigh-Jeans approximation holds and the denominator in (1), $\exp(hf/kT)-1$, may be replaced by hf/kT, thus yielding

$$W\,df = \frac{8\pi kT f^2}{c^3}\,df \qquad \text{joules/m}^3 \qquad (2)$$

The power density emitted P is then obtained by

$$P = \frac{c}{4} W\,df = 2\pi kT \frac{f^2}{c^2}\,df \qquad \text{watts/m}^2 \qquad (3)$$

Thus the expected power density from black-body radiation in a typical frequency interval, e.g. around X-band, may be computed for a given plasma temperature

$$P_T = 10^{-39} T \int_{8\cdot 10^9}^{12\cdot 10^9} f^2\,df = 4 \cdot 10^{-10} T \qquad \text{watts/m}^2 \qquad (4)$$

which amounts to typical values of 0.4 mW/m^2 (= 0.04 $\mu W/cm^2$) for a 10^6 °K plasma. Thus, the contribution from this mode of radiation is usually small for situations of interest in these studies. The power-frequency dependence is further altered since the radiating surface is intercepted by a directional horn. The directivity of such a finite aperture antenna is expressible in terms of an effective intercept area[3]

$$A \propto \frac{1}{4\pi} \frac{c^2}{f^2} \tag{5}$$

from which the power fed to the receiving transmission line may be computed for a one-dimensional geometry

$$P_r = \frac{P}{2} A = kT\,df \approx kT\,\Delta f \tag{6}$$

The factor 1/2 is introduced because the horn accepts only one polarization, the Δf refers to the bandwidth of the receiver used which will vary according to the method of detection adopted. Hence, for the plasma temperature considered above and for a bandwidth of several kMc, the power detected would amount to some 0.03 μW and to even lower values for systems of more reduced bandwidth (Local Oscillator Detectors).

If the plasma configuration is not optically thick, some corrections

are needed to account for the radiation escape.

The ratio of power received, P_r, to that expected from an optically opaque plasma, P_o, can be expressed by adding the contributions over the finite depth of plasma, d.

$$P_r/P_o = \int_o^d \left[\exp(-2\alpha z)\right] d(-2\alpha z) \qquad (7)$$

where α is the attenuation coefficient in nepers/meter which in a first approximation may be assumed constant and uniform over the plasma diameter. In such case, the power received would be

$$P_r = kT\left[1 - \exp(-2\alpha d)\right]\Delta f \qquad \text{Watts} \qquad (8)$$

The absorption coefficient α is, however, a function of collision frequency and depends, therefore, on frequency, density, and temperature of the plasma species. In general, the evaluation of α is difficult and it involves the calculation of the Coulomb collision cross sections for all electron-ion encounters, including excitation processes. The collision frequency per electron, ν_c, for various processes may be defined

$$\nu_c = N_p \overline{\sigma v} \qquad (9)$$

where N_p is the density of the particle type involved in the interaction, $\overline{\sigma v}$ is the collision cross section times velocity for a Maxwellian distribution. Also, the radian plasma frequency, ω_p,

is conventionally defined as

$$\omega_p = (ne^2/m\epsilon_o)^{1/2} = 56.5\sqrt{n_e} \qquad (10)$$

where n_e is the electron density per m^3. For the case of $\nu_c/\omega_p < 0.01$ an approximate relationship for α may be used[4]

$$\alpha \approx \frac{1}{2}\,\frac{\omega}{c}\,\frac{\omega_p^2}{\omega^2}\,\frac{\nu_c}{(\omega^2 - \omega_p^2)^{1/2}} \qquad (11)$$

In the region between 1 and 10 eV the general behavior of the electron collision frequency (or $\overline{\sigma v}$ in formula 9) is strongly dependent on the presence of atoms with low excitation energy, typically copper or aluminum which may be present as electrode materials in the discharge.

In general, for all frequencies below the plasma frequency ω_p, the radiation from the plasma will be similar to that of a black body. However, for frequencies near and above ω_p the bremsstrahlung formula will describe more accurately the power spectrum.

2) The Emission from a Transparent Medium: Bremsstrahlung

The Heitler[5] theory of radiation can be used to evaluate the emission from a population of plasma electrons interacting with the ions under the assumption of a Maxwellian velocity distribution. An electron incident upon an ion distribution will radiate dN photons per unit volume per second into an energy range d(hf), where h is Planck's constant and f the emission frequency

$$dN = n^2 Z^2 \frac{16}{3} \left(\frac{2\pi e^2}{4\pi\varepsilon_o hc}\right) \left(\frac{e^2}{4\pi\varepsilon_o mc^2}\right)^2 mc^2 \left(\frac{2}{m\pi kT}\right)^{1/2}$$

$$\left[\frac{\exp(-hf/2kT)}{hf/2kT} K_o\left(\frac{hf}{2kT}\right)\right] d\left(\frac{hf}{2kT}\right) \qquad (12)$$

where K_o is the modified Bessel function of the second kind[6] as defined

$$K_o(x) = (\log 2 - \gamma)\, I_o(x) - \left\{ I_o(x) \log x - \ldots \right\} \qquad (13)$$

and all other parameters are the conventional notations, all in MKS. The emitted power flow associated with these photons amounts to

$$dP = h \cdot f \cdot dN \qquad (14)$$

This leads to an expression for the total power emitted per unit volume and in a given frequency interval

$$P_t = n^2 Z^2 \quad \frac{e^6}{6hc^3 \epsilon_o^3 m\pi^2} \quad \left(\frac{2\pi kT}{m}\right)^{1/2}$$

$$\int_{hf_1/2kT}^{hf_2/2kT} \exp\left(-\frac{hf}{2kT}\right) K_o\left(\frac{hf}{2kT}\right) d\left(\frac{hf}{2kT}\right) \qquad (15)$$

The evaluation of the constant terms modifies (15) into

$$P_t = 2.46 \cdot 10^{-40} n^2 Z^2 T^{1/2} \left\{ \text{Integral} \right\} \qquad (16)$$

Approximate integration over the typical frequency range 8 - 12 kMc yields

$$P_t = 3.8 \cdot 10^{-40} n^2 Z^2 T^{-1/2} \qquad \text{Watts/m}^3 \qquad (17)$$

For a population of $n = 10^{18}\ m^{-3}$, $T = 10^5\ ^\circ K$, and $Z = 1$, $P_t = 10^{-6}\ W/m^3 = 10^{-6}\ \mu W/cm^3$, which represents a very small amount of power in the frequency range of interest.

3) The Radiation from Gyrating Electrons

i) Single Electron Radiation

It is considered necessary to first evaluate the basic expressions describing the radiation obtainable from a charge moving uniformly on a circle[7, 8, 9]. The gyromagnetic frequency of this motion amounts to

$$f_c = \frac{\omega_c}{2\pi} = \frac{eB}{2\pi m_o \gamma} \qquad (18)$$

where e is the electronic charge, B the magnetic field, m_o the mass of the electron, and γ is the relativistic factor defined by

$$\gamma = (1 - v^2/c^2)^{-1/2} \qquad (19)$$

Upon evaluation of the parameters, the expression reduces to

$$f_c = 2.80 \cdot 10^{10} \frac{B}{\gamma} \qquad (20)$$

When dealing with the nonrelativistic case, $\gamma = 1$ and the expression further simplifies to

$$f_c = 2.8 \cdot 10^{10} \text{ B cycles/sec} \qquad (\text{B in webers/m}^2) \qquad (21a)$$

$$f_c = 2.8 \text{ B (Mc/sec)} \qquad (\text{B in gauss}) \qquad (21b)$$

For convenience of reference this relationship has been plotted in Fig. (1).

It is easy to see that the frequency region of interest in this application, ranging from 1 kMc to 100 kMc, requires the application of magnetic fields ranging from roughly $3.6 \cdot 10^{-2}$ to 3.6 webers/m^2.

In a first analysis, the nonrelativistic approximation is valid. In effect, for electrons of 10 kev the correction for relativistic effects would amount to 2% and for 30 kev to 6% of the uncorrected values. Some additional kinetic parameters are necessary to describe the behavior of the individual electron in a plasma. For the nonrelativistic case the electron velocity is obtainable from the formula

$$eV = mv_e^2/2 \tag{22}$$

which, upon evaluation, yields

$$v_e = 5.93 \cdot 10^5 \sqrt{V} \text{ m/sec} \tag{23}$$

with V in volts. The gyroradius of the electrons on the orbit can now be obtained from the formula

$$r_e = mv/eB \text{ (m)} \tag{24}$$

while in terms of the voltage through which the electron has been accelerated

$$r_e = \frac{3.36 \cdot 10^{-6} \sqrt{V}}{B} \text{ (m)} \tag{25}$$

A 10 kev particle will have, therefore, a velocity of $5.85 \cdot 10^7$ m/sec and a gyroradius of 0.337 mm in a magnetic field of 1 weber/m^2.

The power emitted into radiation can be evaluated by means of the Sommerfeld formula[9]

$$P = (e^2 \omega^4 r^2 / 6\pi \varepsilon_o c^3) \qquad (26)$$

which upon evaluation of the constants yields

$$P = 0.88 \cdot 10^{-54} f^4 r^2 \qquad \text{(Watts)} \qquad (27)$$

For radiation emitted at a frequency of 100 kMc from an electron on a 0.1 mm orbit, a power of $P = 0.88 \cdot 10^{-14}$ watts/electron would be expected. It is convenient to have expressions for the radiative power emitted by an electron in terms of other combinations of parameters than that used in Eq. (27). Listed are pairs of variables, and following them the corresponding expressions (non-relativistic) for the power:

$(v_\perp, B)$	$P = 1.77 \cdot 10^{-31} v_\perp^2 B^2$	watt/electron	(28a)
(T (in kev), B)	$P = 6.22 \cdot 10^{-17} T B^2$	watt/electron	(28b)
$(v_\perp, f_c)$	$P = 2.26 \cdot 10^{-52} v_\perp^2 f_c^2$	watt/electron	(28c)
(T, f_c)	$P = 7.96 \cdot 10^{-38} T f_c^2$	watt/electron	(28d)

For instance, from a population of 10^{18} electrons/m^3 (= 10^{12} cm^{-3}) with a temperature of 1 kev, in a magnetic field of 1 Wb/m^2 (= 10^4 gauss) an emission of $P = 62\ \mu W/cm^3 = 62\ W/m^3$ can be expected. Equations (27) and (28) give the total power radiated by the electron in all directions and in all harmonics of the cyclotron frequency. In many situations it is necessary to know the distribution of the emitted power over direction and over the harmonics. The following expression (developed by Schwinger[10] and Trubnikov[11]) for the power emitted into a unit solid angle making an angle θ with $\bar{B}$ will be used to determine the power in the first harmonic which is emitted (a) parallel to the $\bar{B}$ field and (b) perpendicular to the $\bar{B}$ field. The velocity $\bar{v}$ is assumed to be perpendicular to $\bar{B}$:

$$P_{cn}(\theta) = \frac{e^2 \omega_c^2 \left(1 - \frac{v^2}{c^2}\right) \left(\frac{v}{c}\right)^2}{2\pi c} \left\{ \left(\frac{\cos\theta}{\frac{v}{c}\sin\theta} \right)^2 J_1^2 \left(\frac{v}{c}\sin\theta\right) + J_1'^2 \left(\frac{v}{c}\sin\theta\right) \right\} \tag{29}$$

Thus the power in the first harmonic emitted parallel to the $\bar{B}$ field is ($\theta = 0$, $n = 1$):

$$P_{c1}(0) = \frac{e^2 \omega_c^2}{2\pi c} \left(1 - \frac{v^2}{c^2}\right) \left(\frac{v}{c}\right)^2 \left\{ (1) \left[\lim_{\theta \to 0} \left(\frac{J_1 \left(\frac{v}{c}\sin\theta\right)}{\frac{v}{c}\sin\theta} \right) \right]^2 + \right.$$

$$\left. + \left[\lim_{\theta \to 0} J_1' \left(\frac{v}{c}\sin\theta\right) \right]^2 \right\} \tag{30}$$

Now

$$J_1\left(\frac{v}{c}\sin\theta\right) = \frac{\frac{v}{c}\sin\theta}{2}\left[1 - \frac{\left(\frac{v}{c}\sin\theta\right)^2}{2^2 \cdot 2} + \ldots\right] \qquad (31)$$

and

$$\lim_{\theta \to 0} \frac{J\left(\frac{v}{c}\sin\theta\right)}{\frac{v}{c}\sin\theta} = 1/2 \qquad (32)$$

Also

$$J_n'(x) = \frac{n}{x} J_n(x) - J_{n+1}(x) \qquad (33)$$

and therefore

$$\lim_{\theta \to 0} J_1'\left(\frac{v}{c}\sin\theta\right) = \lim_{\theta \to 0} \frac{1}{\frac{v}{c}\sin\theta}\left[\frac{\frac{v}{c}\sin\theta}{2}\left(1 - \frac{\left(\frac{v}{c}\sin\theta\right)^2}{2^2 \cdot 2} + \ldots\right)\right] = 1/2 \qquad (34)$$

So the power per steradian emitted in the direction parallel to the $\overline{B}$ field is

$$P_{c1}(0) = \frac{e^2 \omega_c^2 \left(1 - \frac{v^2}{c^2}\right)\frac{v^2}{c^2}}{4\pi c} \qquad (35)$$

For non-relativistic velocities this reduces to

$$P_{c1}(0) = \frac{e^2 v^2 \omega_c^2}{4\pi c^3} \qquad (36)$$

in terms of velocity and cyclotron frequency, and to

$$P_{c1}(0) = \frac{e^4 v^2 B^2}{4\pi c^5 m^2} = 2.34 \cdot 10^{-37} v^2 B^2 \qquad (37)$$

in terms of velocity and magnetic field.

The energy radiated into a unit solid angle perpendicular to the magnetic field will now be evaluated (again for the 1st harmonic):

Letting $n = 1$ and $\theta = \pi/2$,

$$P_{c1}(\pi/2) = \frac{e^2 \omega_c^2 \left(1 - \frac{v^2}{c^2}\right) \frac{v^2}{c^2}}{2\pi c} \left\{ \left(\frac{\cos(\pi/2)}{\frac{v}{c} \sin(\pi/2)} \right)^2 J_1^2 \left(\frac{v}{c} \sin \pi/2\right) + \right.$$

$$\left. + J_1'^2 \left(\frac{v}{c} \sin \pi/2\right) \right\} \qquad (38)$$

Or, after simplifying

$$P_{c1}(\pi/2) = \frac{e^2 \omega_c^2 \left(1 - \frac{v^2}{c^2}\right) \frac{v^2}{c^2}}{2\pi c} \left\{ J_1'^2 (v/c) \right\} \qquad (39)$$

Next, write the first few terms of the series expansion of $J_1'(v/c)$:

$$J_1'(v/c) = \frac{1}{\left(\frac{v}{c}\right)} \left[\frac{\left(\frac{v}{c}\right)^2}{2 \cdot 4} + \ldots \right] - \left[\frac{\left(\frac{v}{c}\right)^2}{2^2\, 2!} \left(1 - \frac{\left(\frac{v}{c}\right)^2}{2 \cdot 6} + \ldots\right) \right] \qquad (40)$$

simplifying,

$$J_1'(v/c) \approx \frac{1}{2}\left(1 - \frac{3}{8}(v/c)^2\right) \qquad (41)$$

when we can neglect higher powers than $(v/c)^2$ in the expansion of $J_1'(v/c)$. Therefore,

$$\left[J_1'(v/c)\right]^2 \approx \frac{1}{4}\left[1 - \frac{3}{4}\left(\frac{v}{c}\right)^2 + \left(\frac{3}{8}\right)^2\left(\frac{v}{c}\right)^4\right] \qquad (42)$$

Combining Eq. (42) with Eq. (39), again neglecting higher powers of v/c, we obtain

$$P_{c1}(\pi/2) = \frac{e^2\omega_c^2\left(1 - \frac{v^2}{c^2}\right)\frac{v^2}{c^2}}{8\pi c}\left[1 - \frac{3}{4}\left(\frac{v}{c}\right)^2\right] \qquad (43)$$

For the non-relativistic case we have

$$P_{c1}(\pi/2) = \frac{e^2\omega_c^2 v^2}{8\pi c^3} \qquad (44)$$

For relativistic velocities Eq. (39) should be used instead of Eq. (43). From (36) and (44) the ratio between the power emitted parallel to $\bar{B}$ to that emitted perpendicular to $\bar{B}$ is therefore 2. This is reasonable since parallel to the field one observes two degrees of polarization, and perpendicular to it only one degree.

The distribution of power over the harmonics may be evaluated conveniently by means of a formula suggested by Schwinger[10]

$$\frac{P_{n+1}}{P_n} = \frac{n+2}{2(2n+3)}\left(1 + \frac{1}{n}\right)^{2n+1}\beta^2 \qquad (45)$$

which gives the ratio of power going into the higher harmonics. For the ratio between the fundamental and the second harmonic we obtain

$$P_2/P_1 = 2.4\,\beta^2 \qquad (46)$$

The evaluation leads to the following ratios for several typical energy values

P_2/P_1	E in kev
1.645	400
0.7217	100
0.2587	30
0.0279	3

This indicates that for energies below the 10 kev region no appreciable intensity should be expected in the harmonics and that most of the power will appear in the fundamental.

The above formulae are concerned with the radiation from individual electrons. Although the single electron expressions can be used to obtain an estimate of the total power which will be emitted per unit volume as cyclotron radiation, a more adequate formulation has to be derived to describe the radiation from an electron population in a plasma.

ii) Radiation from a Plasma Electron Population

In arriving at a first estimate of the amount of radio frequency energy which can be expected from a magneto-active plasma certain simplifying assumptions are made. One of these assumptions is that we consider the radiation from an individual electron in the plasma to be that of an electron having a velocity corresponding to the temperature of the plasma in a direction perpendicular to the magnetic field. In reality, the electron velocities are described by a distribution function $f(\bar{r}, \bar{v}, t)$ which as a first approximation may be taken to be Maxwellian.

Another initial assumption which is made is that the electrons radiate as if they were in a vacuum instead of in a magneto-active medium, i.e., the index of refraction n is assumed equal to 1.

The following formula representing a composite treatment of the Sommerfeld-Schott-Eidman work[12] can be utilized in order to obtain the energy radiated by electrons with a cyclotron frequency ω_c as a function of angle in a vacuo:

$$W_s = \frac{e^2 (s\omega_c)^2 \, d\Omega}{2\pi c^3 (1 - \beta_2 \cos\theta)^3} \left\{ v_\perp^2 \left[J_s'\left((s\beta_1 \sin\theta)/(1 - \beta_2 \cos\theta)\right) \right]^2 \right.$$

$$\left. + \left[(c \cos\theta - v_\parallel)/\sin\theta \right]^2 J_s^2 \left((s\beta_1 \sin\theta)/(1 - \beta_2 \cos\theta)\right) \right\} \qquad (47)$$

where

e = electronic charge

c = speed of light

s = order of the harmonic of the cyclotron frequency

θ = polar angle between the direction of the uniform magnetic field and the direction from which we observe the radiation

β_1 = $v_\perp/c$, where v is the velocity component perpendicular to the magnetic field

β_2 = $v_{\parallel}/c$, where v is the velocity component parallel to the magnetic field

W_s = energy emitted per unit time into the solid angle $d\Omega$.

If θ is taken to be $\pi/2$ and s equal to 1 (the fundamental harmonic) then Eq. (47) simplifies to:

$$W_s = \frac{e^2 \omega_c^2 d\Omega}{2\pi c^3} \left\{ v_\perp^2 \left[J_1'(v_\perp/c) \right]^2 + v_{\parallel}^2 \left[J_1 (v_\perp/c) \right]^2 \right\} \qquad (48)$$

In theory this expression can be used in conjunction with the velocity distribution function $f(\overline{r}, \overline{v}, t)$ to give the total energy radiated per unit time at time t in the direction perpendicular to the magnetic field by the electrons in a unit volume located at $\overline{r} = (x, y, z)$. We will proceed as far as possible with this evaluation for the important special case of a

Maxwellian distribution

$$f(v_x, v_y, v_z) = n\,(m/2\pi kT)^{3/2}\ \exp\left[-m(v_x^2 + v_y^2 + v_z^2)/2kT\right]$$

$$= n(m/2\pi kT)^{3/2}\ \exp\left[-m(v_x^2 + v_y^2)/2kT\right]\ \exp\left[-m v_z^2/2kT\right] \tag{49}$$

Multiply Eq. (48) by f, giving

$$W_s(v_\perp, v_{\parallel})\, f(v_\perp, v_{\parallel}) = K_1 \left\{ v_\perp^2 \left[J_1'(v_\perp/c)\right]^2 \right.$$

$$\left. + \ v_{\parallel}^2 \left[J_1(v_\perp/c)\right]^2 \right\}\ \exp\left[-K_2 v_\perp^2\right] \exp\left[-K_2 v_{\parallel}^2\right] \tag{50}$$

where

$$K_1 = (m/2\pi kT)^{3/2}\ n e^2 \omega_c^2\, d\Omega / 2\pi c^3$$

$$K_2 = m/2kT$$

$$v_\perp = (v_x^2 + v_y^2)^{1/2}$$

$$v_{\parallel} = v_z$$

Eq. (50) is now to be integrated over all velocities, but first it must be transformed in several ways. We start by expressing the derivative J_1' in terms of Bessel functions

$$J_1'(v_\perp/c) = 1/2\left[J_0(v_\perp/c) - J_2(v_\perp/c)\right]$$

$$\left[J_1'(v_\perp/c)\right]^2 = 1/4\left[J_0^2(v_\perp/c) - 2J_0(v_\perp/c)\, J_2(v_\perp/c) + J_2^2(v_\perp/c)\right] \tag{51}$$

Next we change from rectangular to cylindrical coordinates in velocity space and therefore need the Jacobian of this transformation,

$$\partial(v_x, v_y, v_z) / \partial(r, \theta, z) = r.$$

Finally the integral $\int_{-\infty}^{+\infty}\int\int W_s \, fd^3\bar{v}$ is broken up into a sum of integrals

$$\int_{-\infty}^{+\infty}\int\int W_s \, fd^3\bar{v} = K_1 \left\{ \int_{-\infty}^{+\infty} \exp\left[-K_2 z^2\right] dz \int_{o}^{+\infty} \int_{o}^{2\pi} r^3 \left[J_1'(r/c)\right]^2 \exp\left[-K_2 r^2\right] dr\, d\theta \right.$$

$$\left. + \int_{-\infty}^{\infty} z^2 \exp\left[-K_2 z^2\right] dz \int_{o}^{2\pi} \int_{o} r\left[J_1(r/c)\right]^2 \exp\left[-K_2 r^2\right] dr\, d\theta \right\} \qquad (52)$$

Since

$$\int_{-\infty}^{\infty} \exp\left[-K_2 z^2\right] dz = (\pi/K_2)^{1/2} \quad \text{and} \quad \int_{-\infty}^{\infty} z^2 \exp\left[-K_2 z^2\right] dz = 1/2(\pi/K_2^3)^{1/2}$$

we have (using Eq. 51)

$$\int_{-\infty}^{+\infty}\int\int W_s \, fd^3\bar{v} = \pi K_1 (\pi/K_2)^{1/2} \left\{ 1/2 \int_{o}^{\infty} r^3 \left[J_o(r/c)\right]^{-2} \exp\left[-K_2 r^2\right] dr - \right.$$

$$- \int_{o}^{\infty} r^3 J_o(r/c)\, J_2(r/c) \exp\left[-K_2 r^2\right] dr + \qquad (53)$$

$$\left. + 1/2 \int_{o}^{\infty} r^3 (J_2(r/c))^2 \exp\left[-K_2 r^2\right] dr + 1/K_2 \int_{o}^{\infty} r (J_1(r/c))^2 \exp\left[-K_2 r^2\right] dr \right\}$$

Each of these integrals is of the type

$$\int_0^\infty J_\mu (at)\, J_\nu (bt)\, \exp(-p^2 t^2)\, t^{\lambda - 1}\, dt \qquad (54)$$

In the present case, where $a = b$, this integral can be evaluated in terms of gamma functions and functions of hypergeometric type[13]

$$\int_0^\infty J_\mu (at)\, J_\nu (at)\, \exp(-p^2 t^2)\, t^{\lambda - 1}\, dt = \frac{a^{(\mu+\nu)}\, \Gamma\left((\lambda+\mu+\nu)/2\right)}{2^{(\mu+\nu)}\, p^{(\lambda+\mu+\nu)}\, \Gamma(\mu+1)\, \Gamma(\nu+1)}$$

$$\left\{ {}_3F_3 \left(\frac{\mu+\nu+1}{2}, \frac{\mu+\nu+2}{2}, \frac{\lambda+\mu+\nu}{2}; \mu+1, \nu+1, \mu+\nu+1; -a^2/p^2 \right) \right\} \qquad (55)$$

The function ${}_3F_3$ is defined in the following manner

$${}_3F_3 (\alpha_1, \alpha_2, \alpha_3; \beta_1, \beta_2, \beta_3; x) = \sum_{n=0}^{\infty} \frac{(\alpha_1)_n (\alpha_2)_n (\alpha_3)_n}{n!\, (\beta_1)_n (\beta_2)_n (\beta_3)_n} x^n \qquad (56)$$

where, by definition, $(c)_n = c(c+1)\ldots(c+n-1)$ for any constant c, and $(c)_o$ is defined to be 1.

As was stated, the complete integral in (53) can be made to depend upon the following definite integrals:

$$I_1 = \int_0^\infty J_o(r/c)\, J_o(r/c)\, \exp(-K_2 r^2)\, r^3\, dr \qquad (57a)$$

$$I_2 = \int_0^\infty J_1(r/c)\, J_1(r/c)\, \exp(-K_2 r^2)\, r\, dr \qquad (57b)$$

$$I_3 = \int_0^\infty J_2(r/c)\, J_2(r/c)\, \exp(-K_2 r^2)\, r^3\, dr \qquad (57c)$$

$$I_4 = \int_0^\infty J_o(r/c)\, J_2(r/c)\, \exp(-K_2 r^2)\, r^3\, dr \qquad (57d)$$

For I_1:

$$\mu = 0,\ \nu = 0,\ \lambda = 4,\ -\frac{a^2}{p^2} = -\frac{1}{c^2K^2}$$

and therefore

$$I_1 = \frac{2!}{K_2^2}\left\{{}_3F_3\left(1/2, 1, 2; 1, 1, 1; -\frac{1}{c^2K^2}\right)\right\} \qquad (58)$$

$$= \frac{2!}{K_2^2}\sum_{n=o}^{\infty} \frac{(1/2)_n\,(1)_n\,(2)_n}{n!\,(1)_n\,(1)_n\,(1)_n}\left(-\frac{1}{c^2K_2}\right)^n \qquad (59)$$

For I_2:

$$\mu = 1,\ \nu = 1,\ \lambda = 2,\ -\frac{a^2}{p^2} = -\frac{1}{c^2K_2}$$

and therefore

$$I_2 = (1/c)^2 \frac{2!}{2^2 (\sqrt{K_2})^4 2!\,!} \left\{ {}_3F_3 \left(\frac{3}{2}, 2, 2; 2, 2, 3; -\frac{1}{c^2 K_2}\right) \right\} \quad (60)$$

$$= \frac{1}{2^2 2!\, c^2 K_2^2} \sum_{n=o}^{\infty} \frac{(3/2)_n (2)_n (2)_n}{n!\, (2)_n (2)_n (3)_n} \left(-\frac{1}{c^2 K_2}\right)^n \quad (61)$$

Similarly, for I_3:

$$\mu = 2,\ \nu = 2,\ \lambda = 4,\ -\frac{a^2}{p^2} = -\frac{1}{c^2 K_2}$$

and

$$I_3 = (1/c)^4 \frac{4!}{(\sqrt{K_2})^8\ 2^4 3!\, 3!} \left\{ {}_3F_3 \left(\frac{5}{2}, 3, 4; 3, 3, 5; -\frac{1}{c^2 K_2}\right) \right\} \quad (62)$$

$$= \frac{4!}{2^4 3!\, 3!\, c^4 K_2^4} \sum_{n=o}^{\infty} \frac{(5/2)_n (3)_n (4)_n}{n!\, (2)_n (2)_n (3)_n} \left(-\frac{1}{c^2 K_2}\right)^n \quad (63)$$

Finally, for I_4:

$$\mu = 0,\ \nu = 2,\ \lambda = 4,\ -\frac{a^2}{p^2} = -\frac{1}{c^2 K_2}$$

and

$$I_4 = (1/c)^2 \frac{3!}{2^2 (\sqrt{K_2})^6 \, 1! \, 3!} \left\{ {}_3F_3 \left(\frac{3}{2}, 2, 3; 1, 3, 3; - \frac{1}{c^2 K_2} \right) \right\} \tag{64}$$

$$= \frac{3!}{2^2 c^2 K_2^3} \sum_{n=0}^{\infty} \frac{\left(\frac{3}{2}\right)_n (2)_n (3)_n}{n! \, (1)_n (3)_n (3)_n} \left(- \frac{1}{c^2 K_2} \right)^n \tag{65}$$

The expressions (59), (61), (63) and (65) which we have derived above, may now be used to replace the integrals I_1, I_2, I_3 and I_4 in the following expression. (essentially Eq. 53):

$$\int_{-\infty}^{\infty}\int\int W_s \, f d^3 \bar{v} = \pi K_1 (\pi/K_2)^{1/2} \left\{ \frac{1}{2} I_1 + \frac{1}{K_2} I_2 + \frac{1}{2} I_3 - I_4 \right\} \tag{66}$$

However, the result of carrying out the substitution is rather cumbersome, so the expression for the power will be left in the form of Eq. (66). Referring to the list of notation given immediately after Eq. (50), the first term in the expansion of Eq. (66) will be given:

$$\int_{-\infty}^{\infty}\int\int W_s \, f d^3 \bar{v} = K_1 (\pi/K_2)^{1/2} \frac{1}{2} \frac{2!}{K_2^2} \tag{67}$$

$$= \frac{n e^2 \omega_c^2 \, kT \, d\Omega}{\pi c^3 m} \tag{68}$$

Eq. (68) gives the amount of power radiated perpendicular to the field lines by a Maxwellian distribution of electrons when higher powers of (kT/mc^2) than the first can be neglected. For higher temperatures more terms in the expansion will be required to give the desired degree of accuracy. The first two terms of the expansion (66), when used to give an estimate of the total power radiated, agree with the results of Trubnikov and Kudryavtsev[14].

REFERENCES

1. J. S. Hey, Nature, 157, 47 (1946).

2. M. K. Planck, "Introduction to Theoretical Physics," MacMillan Co., New York, 1949.

3. M. A. Heald, "The Application of Microwave Techniques to Stellarator Research," Report MATT-17, August, 1959.

4. J. Drummond, "Plasma Physics," McGraw-Hill, 1961.

5. W. Heitler, "Quantum Theory of Radiation," Oxford University Press, 1936.

6. F. Bowman, "Introduction to Bessel Functions," Dover Publications, 1958.

7. L. Landau and E. Lifshitz, "The Classical Theory of Fields," Addison-Wesley, 1959.

8. W. Panofsky and M. Phillips, "Classical Electricity and Magnetism," Addison-Wesley, 1956.

9. A. Sommerfeld, "Electrodynamics," Academic Press, 1952.

10. J. Schwinger, Phys. Rev., 75, 1912 (1949).

11. B. Trubnikov, Soviet Phys. Doklady 3, 136 (1958).

12. V. Ia. Eidman, "The Radiation from an Electron Moving in a Magneto-active Plasma," JETP, 7, 91 (1958).

13. G. N. Watson, "A Treatise on the Theory of Bessel Functions, 2nd Ed.," Cambridge University Press, 1958.

14. B. A. Trubnikov and V. S. Kudryavtsev, 2nd United Nations International Conference on the Peaceful Uses of Atomic Energy, 31, 93 (1958).

II) EXPERIMENTAL STUDIES ON MICROWAVE GENERATION FROM A PLASMA

A) DESCRIPTION OF CONFIGURATION

The basic criteria selected for the design of the experimental configuration were both of a practical and a theoretical nature and were aimed at satisfying the scope of this effort which is to extract microwave energy from the plasma kinetic energy. The key considerations were the following:

i) Special consideration should be given to the production of a high velocity electron population in the plasma with densities around 10^{12} cm^{-3}. This population should be maintained with a minimum of wall and end losses.

ii) A magnetic field should be provided throughout the geometry to decrease radial diffusion losses and, at a particular region within the geometry, to provide the required cyclotron field for the radiating electrons.

iii) For reasons of economy of storage energy, the maximum radial dimensions of the tube should be governed mainly by the ion Larmor radius and should not exceed about three times such parameter for some average ion velocity. The electron gyroradius is much smaller than the ion gyroradius and hence the size of the

current channel is mainly determined by radial electric fields which inhibit diffusive effects.

iv) The magnetic field to be used should be a quasi-DC field, at least with respect to the characteristic times of the discharge current itself, so as to avoid complicating effects due to induced fields. The equipment for the production of a DC magnetic field was not considered necessary for the first phase of this investigation.

The above requirements led to the selection of a Penning-type geometry (PIG = Penning Ionization Gauge) for the radiator[1]. The schematic cross-section of the apparatus is presented in Figure 2 and the physical embodiment of the geometry together with all the ancillary apparatus is rendered in Photographs 3a and 3b.

The configuration consists of two cathodes located at the end of the tube and two annular anodes centrally positioned. In this geometry the electrons will oscillate between the two cathodes due to the centrally symmetric profile of the electric field and at the same time diffusive losses of the electrons will be prevented by the longitudinal magnetic field. The strong Lorentz forces acting on the electrons will cause the appearance of radial electric fields acting so as to impede ion diffusion to the walls.

The relative spacing between anode and cathode can be adjusted bilaterally

by sliding the supporting stainless steel rods through appropriately located vacuum seals. The vessel can be initially evacuated by means of a mechanical pump and a 2" diffusion pump. The pressure is then selected to allow operation in a regime where the electrons can complete a number of gyro-orbits before undergoing collisions. This pressure is maintained dynamically by adjusting a regulating leak valve, thus achieving equilibrium at the desired point.

B) OPERATION OF THE RADIATOR SYSTEM

The complete system developed to study the emission of cyclotron radiation consisted of the following main components:

i) The discharge vessel, associated vacuum equipment, capacitor bank providing discharge current and associated electronics.

ii) The magnet coils with Helmholtz gap for detection of the emitted radiation, the capacitor bank for energizing the coils and the associated triggering electronics.

iii) The microwave detection equipment and associated electronics; in this particular study, X-band and K-band equipment was used for the detection of the emitted radiation.

The schematic outline of the operation of the electronic components of these subsystems is given in Figure 4.

The operation of the above three main components involved the following details and the knowledge of several pertinent parameters:

i) The pressure in the discharge vessel was selected according to the criterion listed under A. This usually involved a range of pressures below 30 microns in argon or air. Argon was used during the initial runs, but more repetitively consistent results were obtained when working in air. The breakdown conditions were simpler and satisfactory discharge patterns could be obtained already at voltages as low as 4 kV with a 6 cm cathode-anode spacing (see Fig. 2). A large portion of the data presented was run at around 18 microns Hg. The cathodes were usually held at ground potential, as a safeguard against unwanted breakdowns into the vacuum equipment, and the anodes were pulsed positively with voltages up to 20 kV. A capacitor bank of 15-45 μf (variable in steps) provided the sinusoidal discharge current which could be monitored by inserting a Rogowski loop around the conductor to the cathode and integrating the signal. The peak current was then computed from the knowledge of the rise-time τ_r, which amounted to 10 μsec. Thus, $I_p = \pi CV/2\tau_r =$ 2.55 kA/kV for the 15 μf case, corresponding to a typical current of 22,500 A at 10 kV. The tube was run during these experiments in a single-shot regime and no attempt was made to obtain any

finite repetition rate because of the experimental nature of this phase. The pulse for firing the ignitron circuit of this bank was obtained from a time delay generator set to trigger at the peak of the magnetic field pulse, when $\dot{B} \approx 0$. The current through the discharge lasted about 2 cycles or nearly 80 μsec.

In general, brass anodes were found preferable to stainless steel anodes which exhibited some sputtering during operation. Such condition would require intermittent cleaning of the tube to avoid internal attenuation of the radiation emitted. The possibility of using high voltage lines instead of capacitors in the future will appreciably shorten the pulse in time and hence decrease the dissipative and erosive effects.

ii) The magnetic field was provided by two single-layer, 10-turn solenoids connected in series. The inductance was around 3.4 μH and, when connected to a bank of 800 μf, the risetime was about 100 μsec. This resulted in peak currents of $I_p = 12$ kA/kV.

Small magnetic pick-up probes were used to investigate the longitudinal and radial field profiles. A typical profile is presented in Fig. 5 for a spacing of 2.50 cm between the two coils. A field ratio of 2 : 1 is obtainable between the field in the coil and the field

at the center of the gap. For operation at X-band, requiring a field of 3.57 kG for 10 kMc, the bank had to be charged to 1.0 kV corresponding to a stored energy of 400 joules. Thus the magnetic field at the center of the gap could be set with sufficient accuracy by adjusting the voltage on the capacitor bank. The signal for triggering the two ignitrons used to switch the bank was derived from a master trigger starting the firing sequence (see Fig. 4).

iii) The radiation emitted orthogonally to the magnetic field lines is plane polarized. Appropriately, a horn is located close to the discharge vessel with the E-field aligned to propagate in the TE_{10} mode. The microwave signal is then fed through some 10 feet of waveguide into a screen cage where the detection equipment is located. The pulse is usually fed over a Uniline, a variable attenuator, and finally into a crystal detector. From here the signal is fed to a wide-band preamplifier (Tektronix type L) with a 52 Ohm termination resistor.

The detection of the signal was greatly hindered by the introduction of an objectionable amount of noise into the trigger line of the CRO. After a number of different attempts, an expedient remedy was found by picking up an optical signal as a trigger from the discharge of a 5C22 thyratron in the delay trigger circuit. The

optical pulse was fed through an optical line into the cage and detected there by a 931 photomultiplier whose output was used to trigger the scope. Adopting this method, the noise level could be decreased well into the region of some 100 microvolts.

During the initial phase of the experiments, attempts were made to detect the expected radiation pulse by narrow-band methods. A local oscillator was introduced and mixed with the incoming pulse in a magic tee. The output was then sent through several stages of amplification. These attempts were, however, not successful because of the noise level encountered (which at such time had not been cured by the introduction of the optical trigger) and possibly also because the signal is exhibiting some frequency spread around f_c. This last effect is ascribable to the field distribution over the radiating region and possibly also because of the effect of the field B_θ produced by the discharge current I_z. The crystal used for detection at X-band was a 1N23B with a nominal impedance of 400 Ohms, and a 1N26 for the detection at K-band with a nominal impedance of 500 Ohms.

C) RADIATION DETECTION AT X-BAND

A number of runs were carried out under carefully controlled conditions both at X-band and, later on, at K-band. The data could be secured after all disturbing effects of extraneous pick-up and noise had been eliminated. During these runs, three parameters were varied and the effects of these changes were detected in terms of the power output. The parameters were: the strength of the magnetic field, the externally applied electric field (and hence also the peak current), and the ambient pressure. For sake of simplicity only results at two pressure points will be quoted, namely at 20 and 30 microns Hg.

In the proper time sequence, the magnetic field is fired first and set to reach at field maximum the predetermined value H_c, the cyclotron resonance field, at the center of the gap. This takes about 100 μsec. The time delay is properly set to prefire the ignitron triggering circuit, so that the discharge occurs precisely at the peak of the magnetic field. Since the risetime of the discharge is about 10 μsec, little or no field change occurs during such interval. The observed microwave pulse output starts soon after the initial rise of the longitudinal discharge current and is usually back to zero before the time of maximum current. In general, the pulse is only some 0.2 - 0.4 μsec wide, as can be seen from a typical series of shots presented in pictures 13a, 13b, and 13c. The precise temporal location of this pulse with respect to the current

pulse has not yet been obtained because the introduction of the current pulse pick-up into the cage is always accompanied by an undesirable amount of noise which obscures the microwave signal.

The attempt has been made to detect the emitted signal together with a transmission pattern. To this purpose a 9.75 kMc klystron system was fed via waveguides underneath the gap between the coils and the horn was directed to radiate through the plasma discharge into the pick-up horn. The signal detected under these conditions is presented in Fig. 14, from which it can be seen that the plasma reaches a quasi-opacity regime within the risetime of the discharge. It appears that the signals detected in these experiments lie immediately before the onset of opacity. Further tests would be needed to establish this point with certainty.

The power output from the plasma was measured as a function of magnetic field and the data are presented in Figs. 6 and 7 for discharge voltages ranging from 5 to 10 kV. The center frequency of the passband, namely 10 kMc, is indicated with an arrow. It should be stressed that these results do not give any indication regarding the frequency spread of the output signal, they are merely a function of the output from the radiator as modified by the finite acceptance function of the microwave system. Since the output signal is expected to rise as B^2, the initial rise in power output is completely understandable if we bear in mind the acceptance versus frequency of the X-band hardware.

The fall-off beyond the center-frequency is less steep because the signal output keeps increasing with the field. A more extended power output versus magnetic field graph is given in Fig. 8 for a constant discharge voltage of 8 kV. The general behavior encountered in the results of Figs. 6 and 7 is still evident. The detection of power in the higher frequency region is explainable because of the finite attenuation coefficient which has no set cut-off point. Similar data were gathered at 30 microns Hg pressure for discharge voltages of 6, 8, 10 kV (see Fig. 9). Although the general trend of the power output remains the same, it is noticeable how much lower the output is at the lower magnetic fields. This is understandable because the collisions during any gyro-orbit start influencing the radiative output.

The peak power was also investigated as a function of discharge voltage for a constant magnetic field. The results are given in Fig. 10 and show a trend of at least a linear increase with the applied electric field.

In all these measurements, the nominal detectivity of the crystal was assumed to be 0.4 μA/μW corresponding to the impedance of 400 Ohms at 9.37 kMc/s. The presented values of the power are somewhat in doubt, pending absolute calibration procedures because of effects due to the termination. However, it is felt that they represent lower limits and that possibly

5 times higher powers could have been extracted from the radiator. For instance, the peak power detected at X-band could run from a minimum value of 52 mW to a maximum of about 250 mW. On Fig. 10 (and all other figures) the low values have been entered.

D) MEASUREMENTS AT K-BAND

It was felt to be of interest to explore the power emission by this mechanism also at K-band. The power detected as a function of magnetic field is given in Fig. 11 and the power as a function of discharge voltage for a constant magnetic field is presented in Fig. 12.

The interesting feature of Fig. 11 is that two peaks become discernible. The first peak appears at magnetic field values typical for the frequencies around X-band, namely about 10 kMc/s, the second peak appears around frequencies slightly above the center-frequency of the K-passband. It is hypothesized that the first peak represents the second harmonic of the radiation output corresponding to the magnetic fields at X-band, and that the second peak belongs to the fundamental output at K-band. The relative values of these outputs would seem to be in quantitative agreement.

The behavior of the power output versus discharge voltage seems to be in general agreement with the findings at X-band.

The typical radiation signal detected at K-band is presented in pictures 15a, 15b, 15c.

Also for these results, lower limits for the radiative output have been entered in the graphs. Therefore, the typical values would range from about 50 mW to a possible 250 mW.

REFERENCE

1. Z. M. Penning, Physica, 3, 873 (1936); 4, 71 (1937).

III) DISCUSSION OF RESULTS

With fields of 3.6 kG, power outputs at X-band (approximately 10 kMc) as high as 200 mW have been observed. In order to understand this amount of microwave power, we notice first that apparently only cyclotron radiation can account for the observed power in this frequency band. If we first assume that the radiation is incoherent, we may write (where 511 is the rest energy of an electron in keV):

$$200 \cdot 10^{-3} = nVE_{\perp}\ 8.05 \cdot 10^{-18} \left[1 - \frac{(E_{\perp} + E_{\parallel})}{511}\right] \qquad (1)$$

or assuming $E_{\perp} + E_{\parallel} << 511$,

$$nVE_{\perp} = 2.48 \cdot 10^{16} \qquad (2)$$

Now in this experiment, if we assume there are no accelerating mechanisms within the plasma, the highest energy attainable is the applied voltage, which in the case discussed was 10 kilovolts. Also the maximum volume which may be involved is 4 to 5 cm^3. Hence, the density must be at least

$$n \geq \frac{2.48 \cdot 10^{16}}{10 \cdot 5} = 4.97 \cdot 10^{14}/cm^3 \qquad (3)$$

We note that this density is greater than the critical density for a transparent plasma at 10 kMc, so that the plasma must be a surface radiator rather than a volume radiator ($\lambda \leq 7$ mm).

In such a case, we have

$$200 \cdot 10^{-3} = 4.28 \cdot 10^{-12} \frac{A\sqrt{n}}{\sqrt{1 - \frac{n_o}{n}}} \qquad (4)$$

or that (since $n >> n_o$)

$$n > \frac{2.18 \cdot 10^{20}}{A^2} \text{ electrons/cm}^3 \qquad (5)$$

For the case we are considering, if all of the ions were <u>fully</u> ionized ($Z = 15$), the maximum electron density is $2 \cdot 10^{16}/\text{cm}^3$, so we have for A

$$A \geq \sqrt{\frac{2.18 \cdot 10^{19}}{2 \cdot 10^{16}}} = 34.7 \text{ cm}^2 \qquad (6)$$

which is at least 3 or 4 times the available radiating surface area in the geometry used. If we assume a lower energy per electron than the maximum applied voltage, the figures lead to even more impossible results. Hence, one of our assumptions must be wrong.

We list below, in reverse order, our assumptions made in the above calculations, and examine them in the order listed.

1. <u>Radiating area</u> is no larger than 10 cm^2. $A \leq 10 \text{ cm}^2$.

   This is fixed by the geometry of the apparatus and seems a very liberal estimate of the radiating area rather than a conservative one.

2. Plasma is fully ionized. $Z \leq 15$.

This is surely the maximum possible density attainable, for it says every electron in the device is a free electron.

3. Radiating volume is no greater than 5 cm^3. $V \leq 5$.

Again, the geometry limits the volume, and even three times this liberal estimate leads to the surface radiator problem.

4. Energy is no greater than 10 keV $E_\perp \leq 10$.

If there are no accelerating mechanisms at work within the plasma, the applied voltage is the upper limit to the energy any appreciable number of electrons may have. All other external sources of energy are relatively inefficient and might impart 10 - 100 eV to the electrons at maximum. If we choose to assume a higher electron energy, we must postulate some acceleration scheme in the plasma which we may denote as Alternative 1.

5. Electrons radiate incoherently. $p = nV\epsilon$.

It is difficult to conceive of any forces which would tend to bunch the electrons and leave them bunched for a cyclotron period so that they would radiate coherently. In spite of the conceptual difficulty, we might postulate such a mechanism and denote it Alternative 2.

Now in addition to the two alternatives listed above, we might consider some other alternatives.

Alternative 3: Plasma not opaque for $\omega < \omega_p$.

If we consider propagation perpendicular to the magnetic field, rather than along the field lines, there is one weakly coupled wave which cuts off at $\omega_p/\sqrt{2}$ instead of ω_p for $\omega = \omega_c$, the cyclotron frequency. This does not alter the picture much, and probably this mode plays a minor role anyway. We might make a more drastic assumption that due to some non-uniformity in the plasma, radiation at the cyclotron frequency does penetrate the plasma. If the possibility is allowed, however difficult conceptually, the matter of the duration of the pulse is difficult to account for, inasmuch as there is no clear reason why the pulse should last .1 μsec if the radiation is due to an unattenuated volume-radiating plasma. If the plasma is assumed to be momentarily transparent, it could not conceivably remain transparent for more than the order of 10 or even 100 periods of the plasma oscillations, and at the density required to account for the signal amplitude, the period is $1.5 \cdot 10^{-11}$ sec, so that the supposed transparency could hardly be expected to last more than 1 ns, a factor of 100 shorter than observed.

Alternative 4: It was assumed throughout the course of the experiment that the radiation was cyclotron radiation. Although apparently reasonable estimates disallow all other types of radiation as even less likely than cyclotron radiation, we may have observed some new type of radiation phenomena which was not considered. This seems highly unlikely and this alternative will not be considered further.

If we now return to Alternative 2, and make some ad hoc assumptions about bunch sizes, we can see some of the possibilities and difficulties with this idea. First, we consider bunches of N electrons with radius a and density n. Then we have $N = \frac{4\pi}{3} a^3 n$ and we demand that $a << r_L$ (Larmor radius $= r_L$). If we assume that there are K bunches, then to account for the observed power, we have

$$KN^2 = 2.48 \cdot 10^{15}/E_\perp \qquad (E_\perp + E_\parallel << 511) \qquad (7)$$

If we let $E_\perp = 1$ keV, $n = 10^{12}$/cc, $a = 10\mu$ ($r_L = 300\sqrt{E_\perp}\mu$), then $N = 4.2 \cdot 10^3$ and $K = 1.4 \cdot 10^8$. In this case

$$KN = 5.91 \cdot 10^{11} \text{ particles at 1 keV} \qquad (8)$$

so that the active radiating particles would represent 6% of the electrons in a 5 cc plasma with average density $n_e = 2 \cdot 10^{12}$/cc, and such a plasma is still essentially transparent to the radiation at 10 kMc. If we allow the electrons to

have a higher coherent average energy, we need only suppose a correspondingly lower percentage of the total number of electrons are involved. Any decrease in size or internal density of the bunches will make the total number of electrons involved increase very rapidly, however, and the experimental evidence seems to indicate that the overall average density is no more than $2 \cdot 10^{12}$ or so at the time of the power burst. Since we have no model for what might cause such bunching, it is difficult to think of a crucial experimental test which would prove or disprove the ad hoc hypothesis.

The only other alternative is that ofassuming some accelerating mechanism in the plasma so that we are not limited to 10 keV electrons (Alternative No. 1). In this regard, we note that in a plasma in a magnetic field with only 5 - 20 kilovolts applied, X-rays have been observed with energies as high as 100 keV[1, 2, 3]. If we postulate some such similar mechanism is operating in our plasma, we can account for the results with a density of only $5 \cdot 10^{12}$/cc, and lower for higher energies yet. T. H. Stix has suggested a mechanism for such an acceleration and his results indicate that these energies could easily be attained in .1 μsec[4]. In that report, electrons are accelerated by a beam-plasma overstability which leads to the buildup of large oscillating fields near the plasma frequency. When the plasma frequency approaches the cyclotron frequency, the electrons are quickly accelerated to these very high energies. The energy gained is transverse to the magnetic field, leading to an $E_{\perp} >> E_{\parallel}$, so that electrons accelerated in such

a system should show strong cyclotron radiation. In addition, his computations show that for higher densities where the plasma frequency is near a harmonic of the cyclotron frequency, the overstability drives the electrons in a similar manner. A typical case where $\omega_c = \omega_p$, beam energy = 10 keV ($E_{||} = 10$), plasma mean energy = 20 eV, the acceleration time to 100 keV perpendicular to the field ($E_{\perp} = 100$) is .095 μsec, which agrees well with our characteristic times. The rapid decay of the signal could be due to the increasing plasma density so that the overstability no longer drives the electrons until it is double the critical value for the fundamental. Some small bumps in the radiation pattern have appeared, and these may be due to harmonics, to which the X-band equipment was relatively insensitive. This mechanism presupposes a very turbulent and non-linear plasma in a magnetic field, and the beam which is used to drive the acceleration is present during the early, turbulent, and non-linear portion of our discharge. If this is the proper explanation, we would expect to find 100 keV X-rays with a scintillator detector, and such a search should prove crucial to this explanation. Also, if X-band and K-band equipment were used simultaneously, the fundamental should appear and disappear in the X-band detector before the first harmonic appeared in the K-band equipment due to the rising density. If this did occur, it might also prove to be a crucial test of the theory as accounting for the observed radiation.

REFERENCES

1. L. F. Karchenko, Ya. B. Fainberg, R. M. Nikolayev, E. A. Kornilov, E. I. Lutsenko and N. S. Pedenko, Nuclear Fusion, 1962 Supplement, Part III, 1101.

2. I. Alexeff, R. Neidigh, W. F. Peed, E. D. Shipley and E. G. Harris, Phys. Rev. Letters, 10, 273 (1963).

3. L. D. Smullin and W. D. Getty, Phys. Rev. Letters, 9, 3 (1962).

4. T. H. Stix, Project Matterhorn Report, Matt-239, February, 1964.

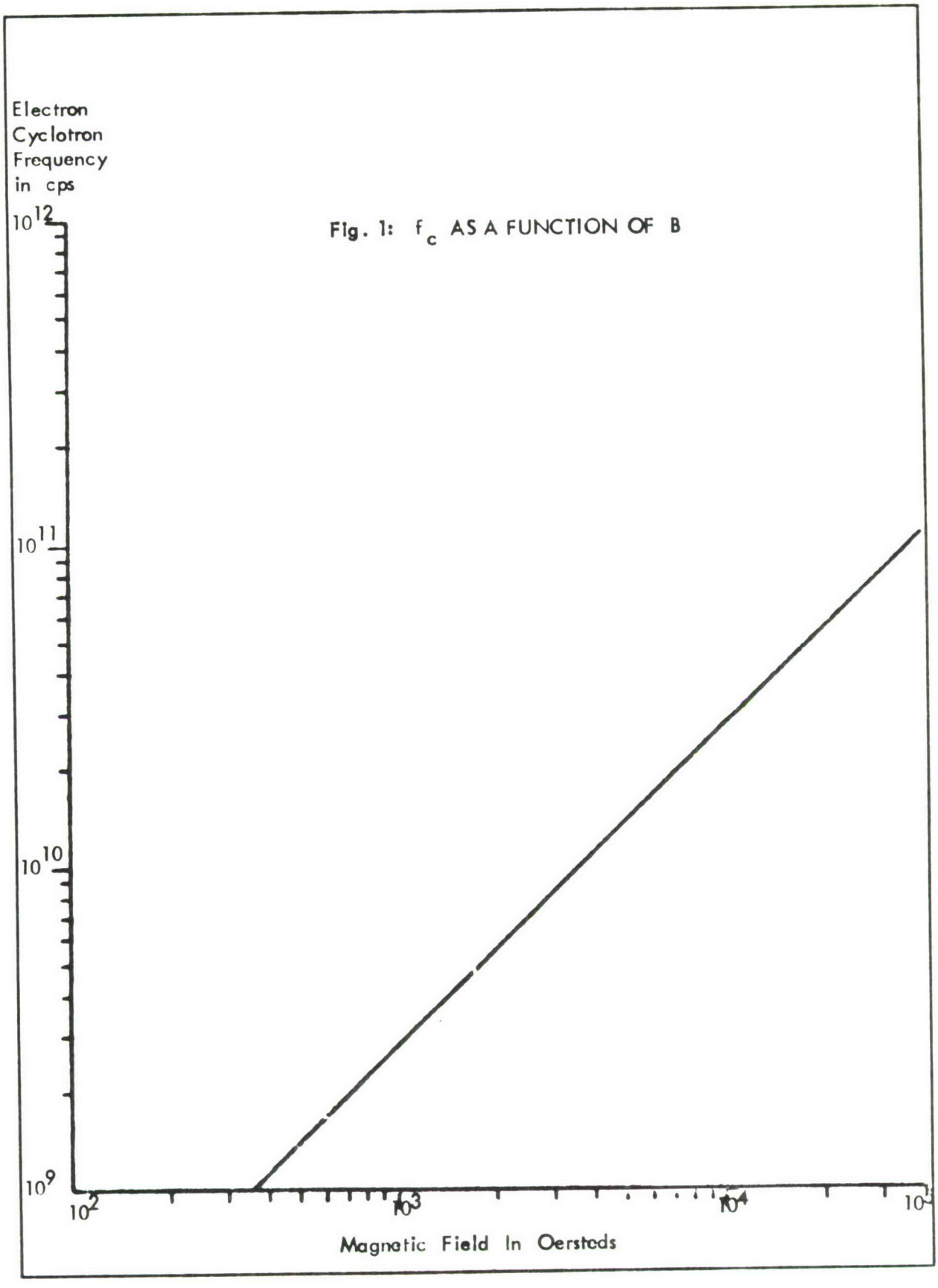

Fig. 1: f_c AS A FUNCTION OF B

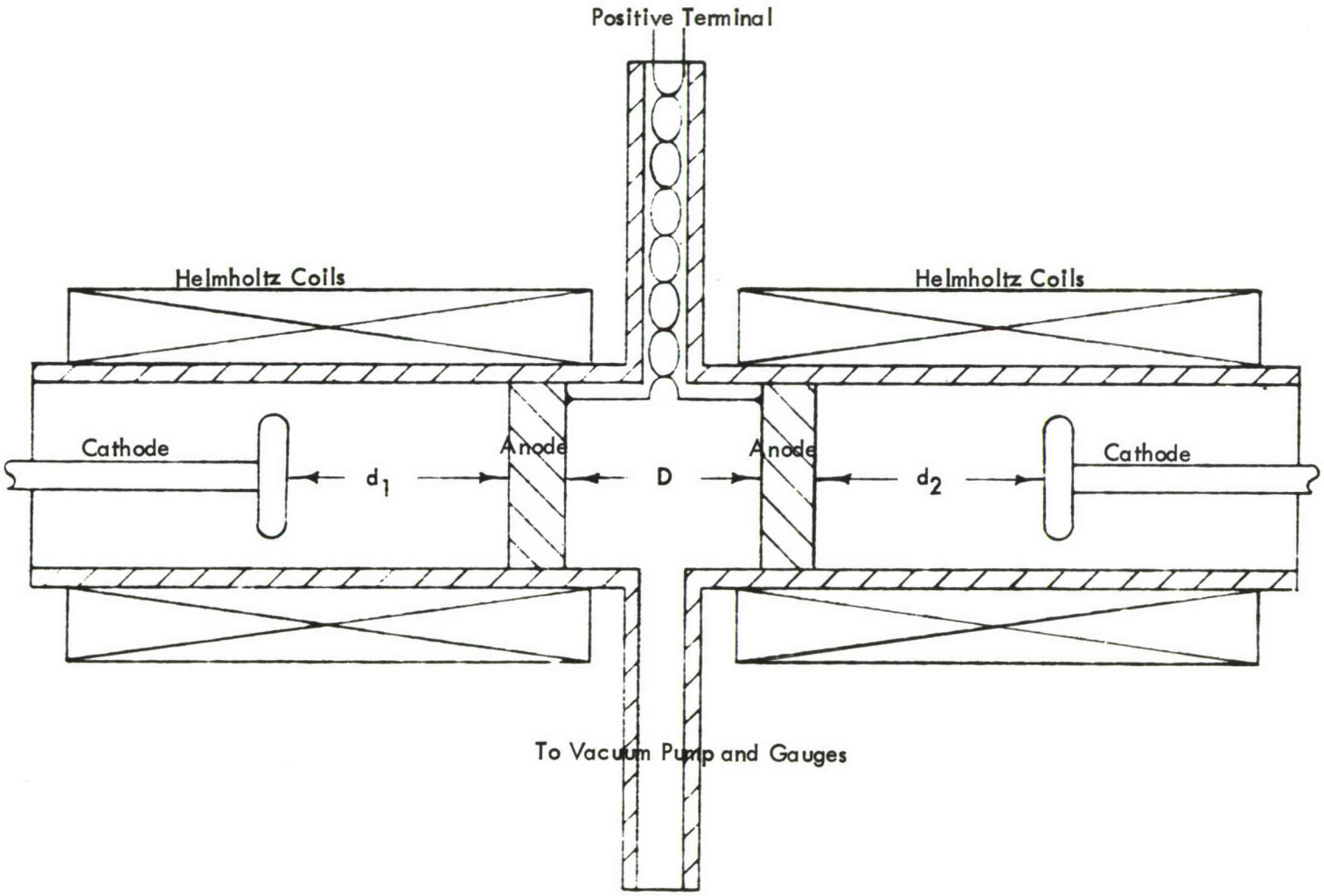

Fig. 2

SCHEMATIC CROSS SECTION OF RADIATOR GEOMETRY

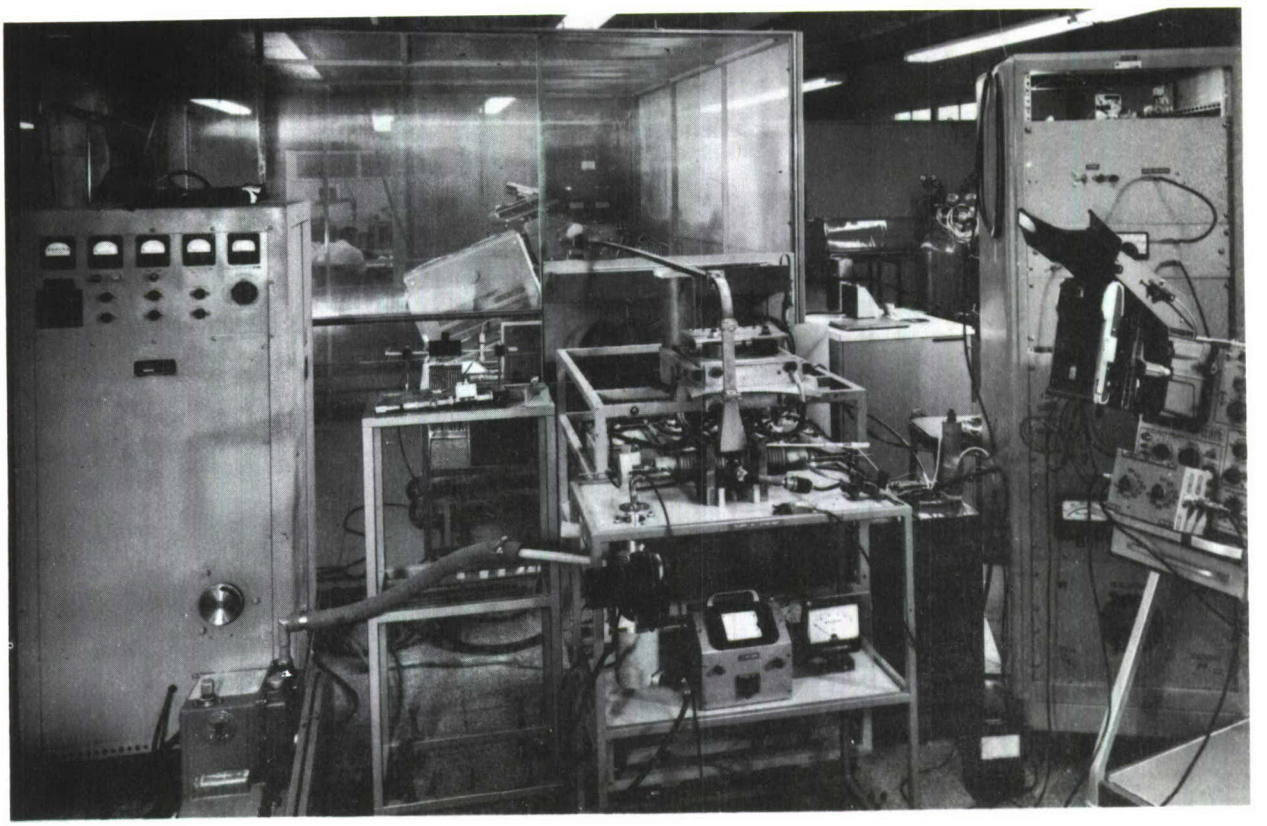

Fig. 3a: Cyclotron Radiator with Ancillary Equipment and Detection Hardware at X-band.

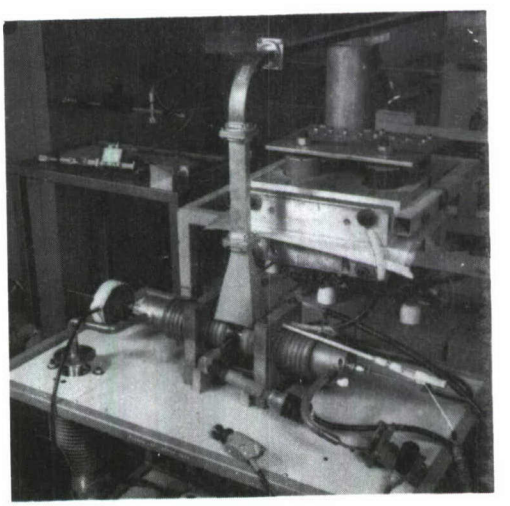

Fig. 3b: Detailed View of Radiator, Magnet Coils, Rogowski Loop, Magnetic Pick-up Coil and Vacuum System.

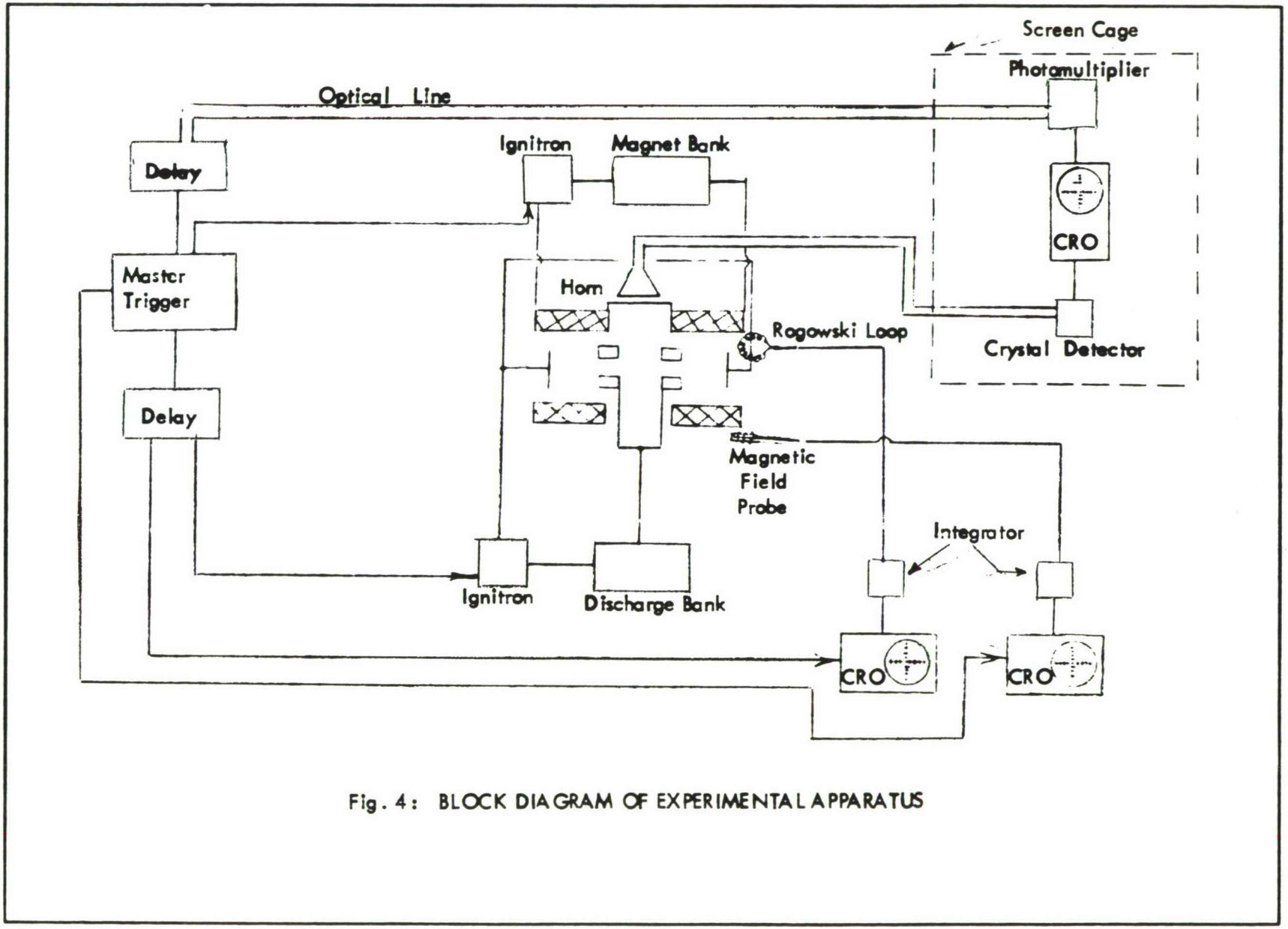

Fig. 4: BLOCK DIAGRAM OF EXPERIMENTAL APPARATUS

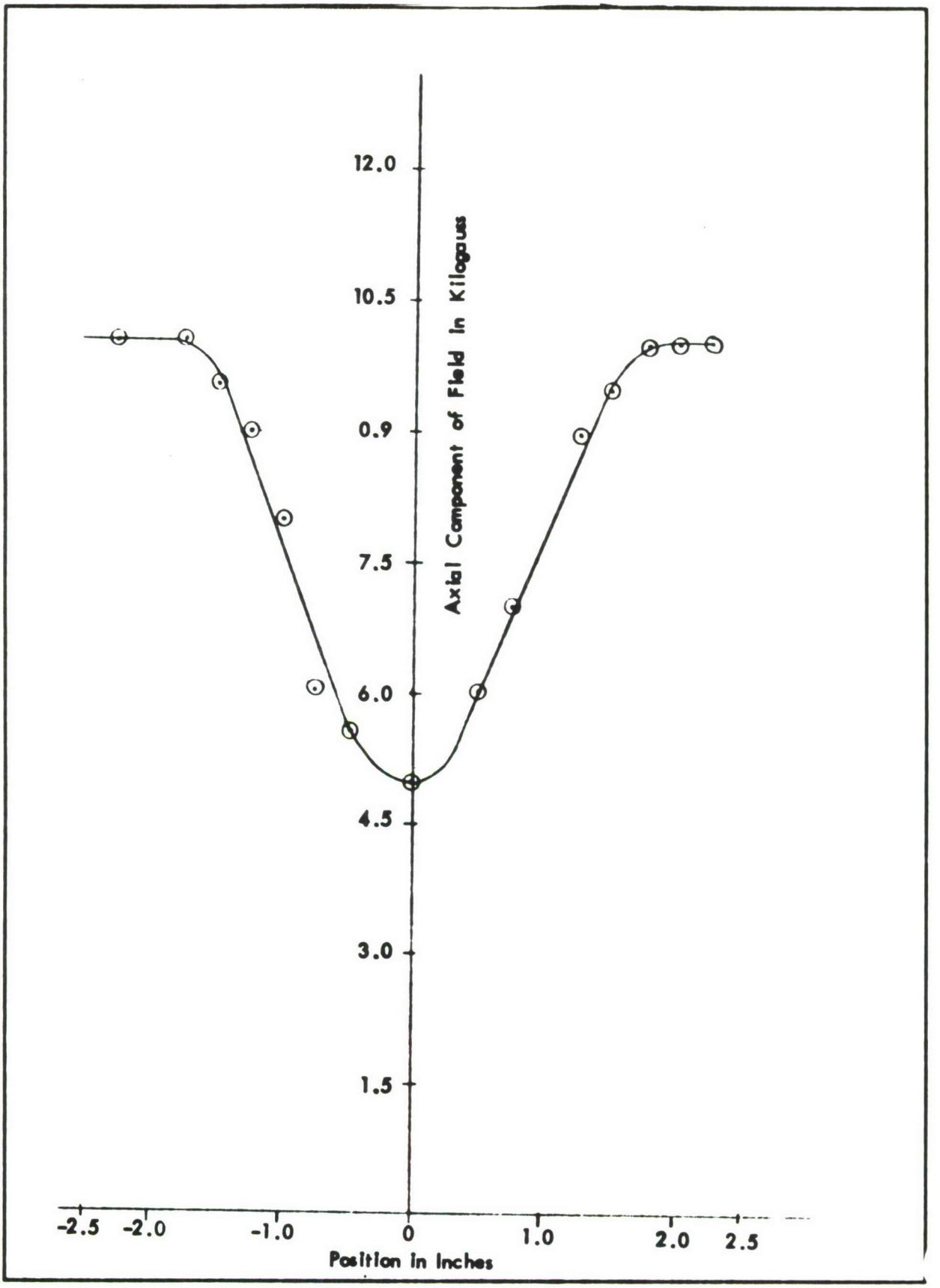

Fig. 5: PROFILE OF AXIAL FIELD FOR COILS IN SERIES WITH A SPACING OF 0.98".

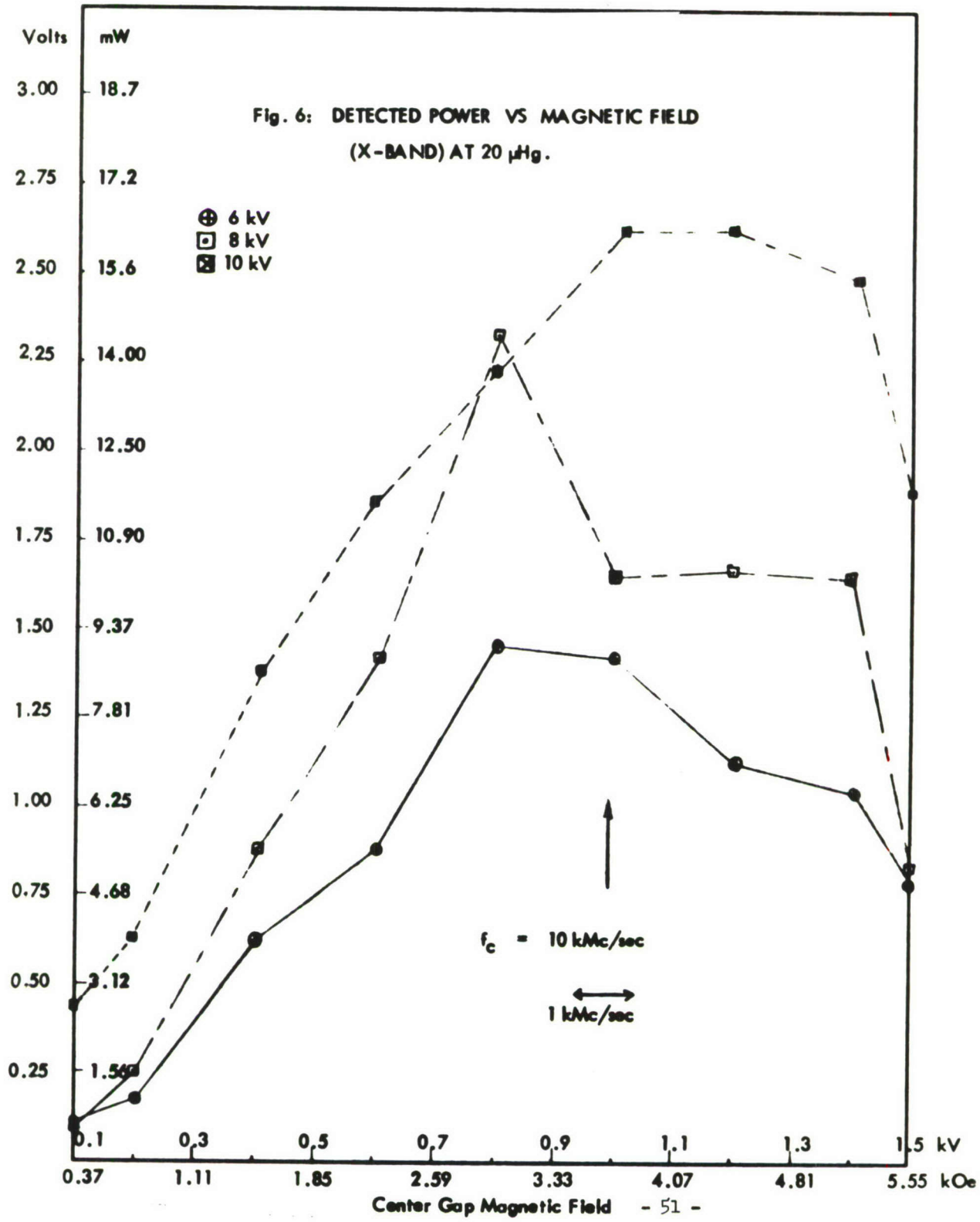

Fig. 6: DETECTED POWER VS MAGNETIC FIELD (X-BAND) AT 20 μHg.

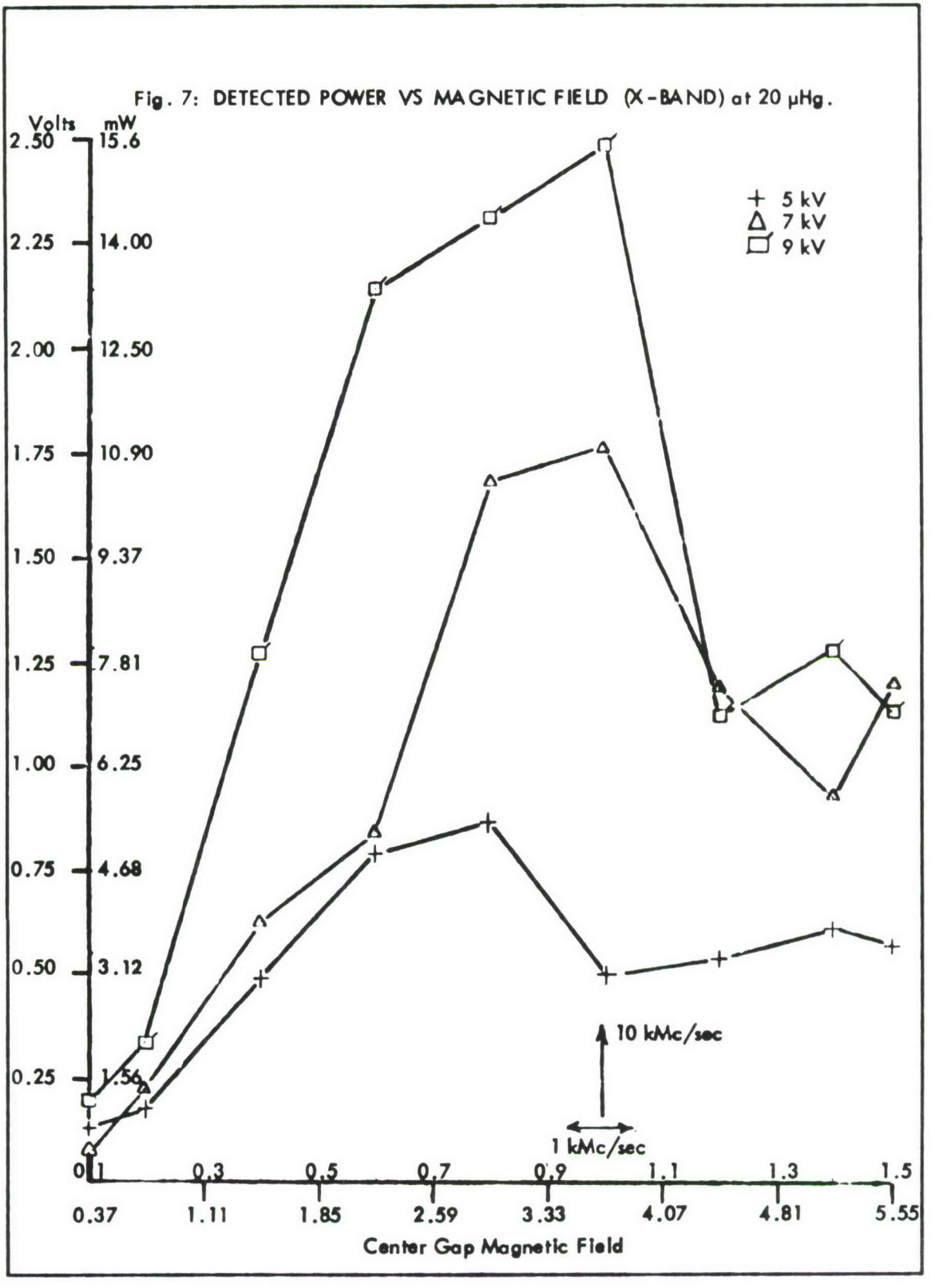
Fig. 7: DETECTED POWER VS MAGNETIC FIELD (X-BAND) at 20 μHg.
Volts
mW
2.50
15.6
2.25
14.00
2.00
12.50
1.75
10.90
1.50
9.37
1.25
7.81
1.00
6.25
0.75
4.68
0.50
3.12
0.25
1.56
+ 5 kV
Δ 7 kV
□ 9 kV
10 kMc/sec
1 kMc/sec
0
0.3
0.5
0.7
0.9
1.1
1.3
1.5
kV
0.37
1.11
1.85
2.59
3.33
4.07
4.81
5.55
kOe
Center Gap Magnetic Field

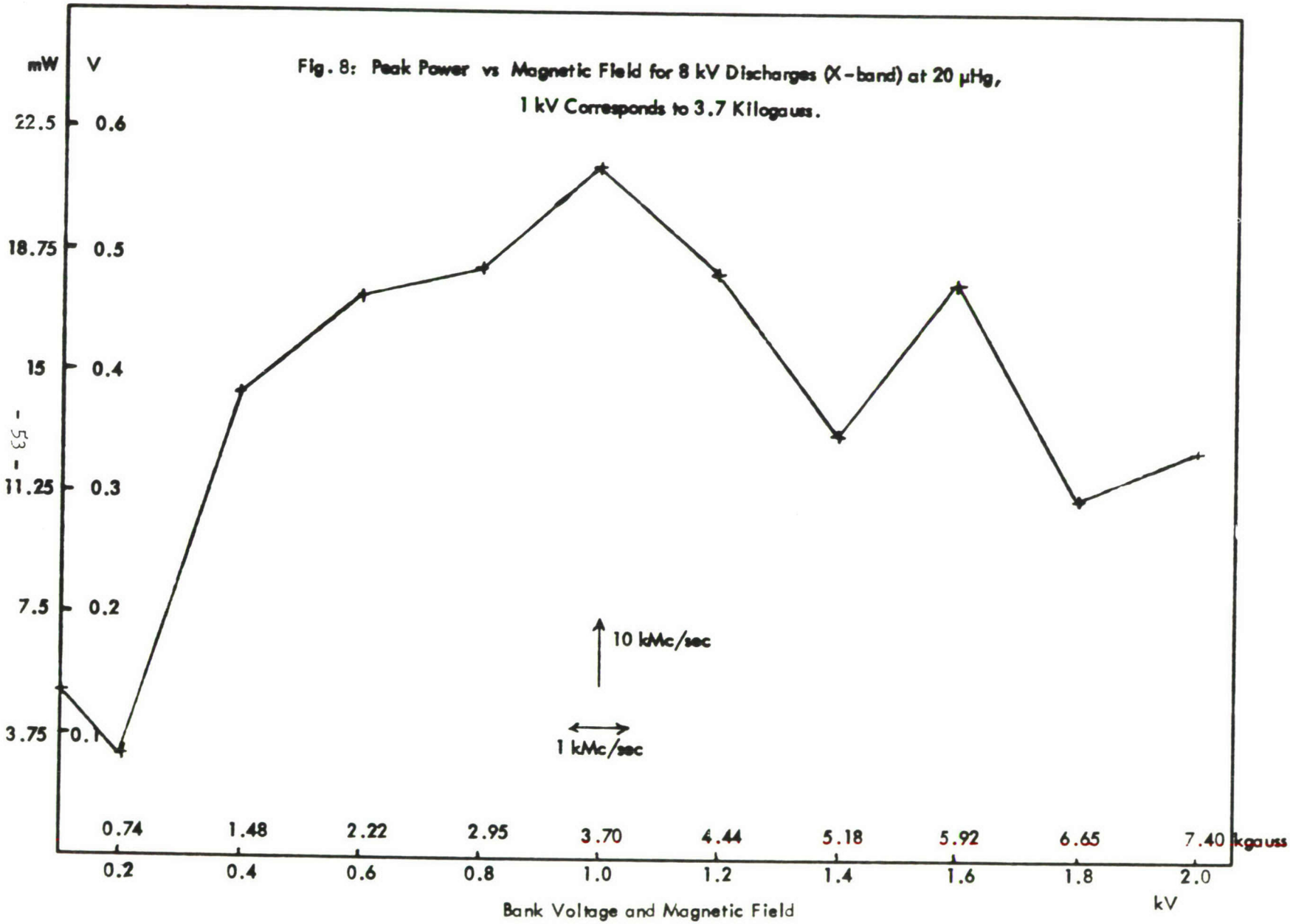

Fig. 8: Peak Power vs Magnetic Field for 8 kV Discharges (X-band) at 20 μHg,
1 kV Corresponds to 3.7 Kilogauss.

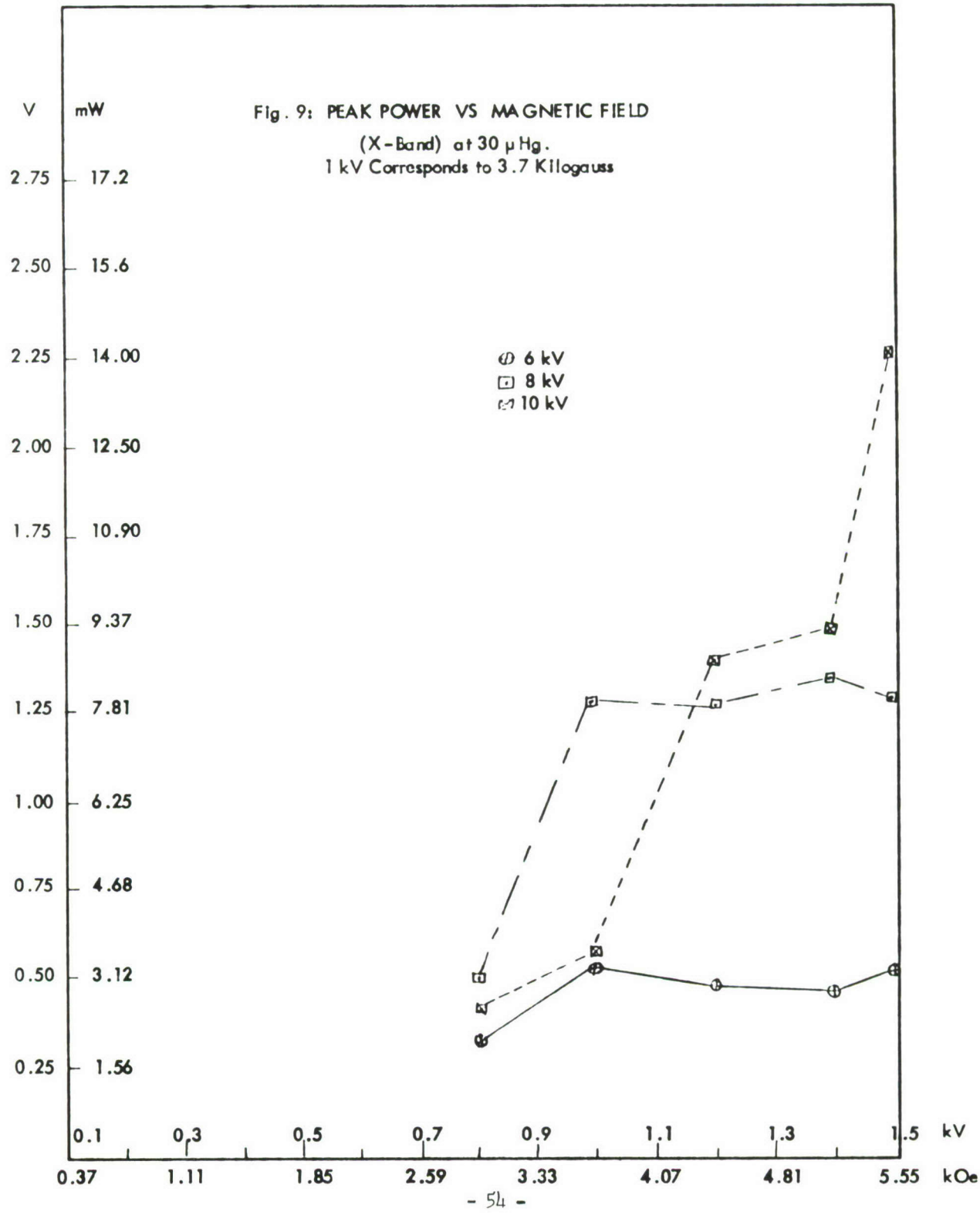

Fig. 9: PEAK POWER VS MAGNETIC FIELD
(X-Band) at 30 μ Hg.
1 kV Corresponds to 3.7 Kilogauss

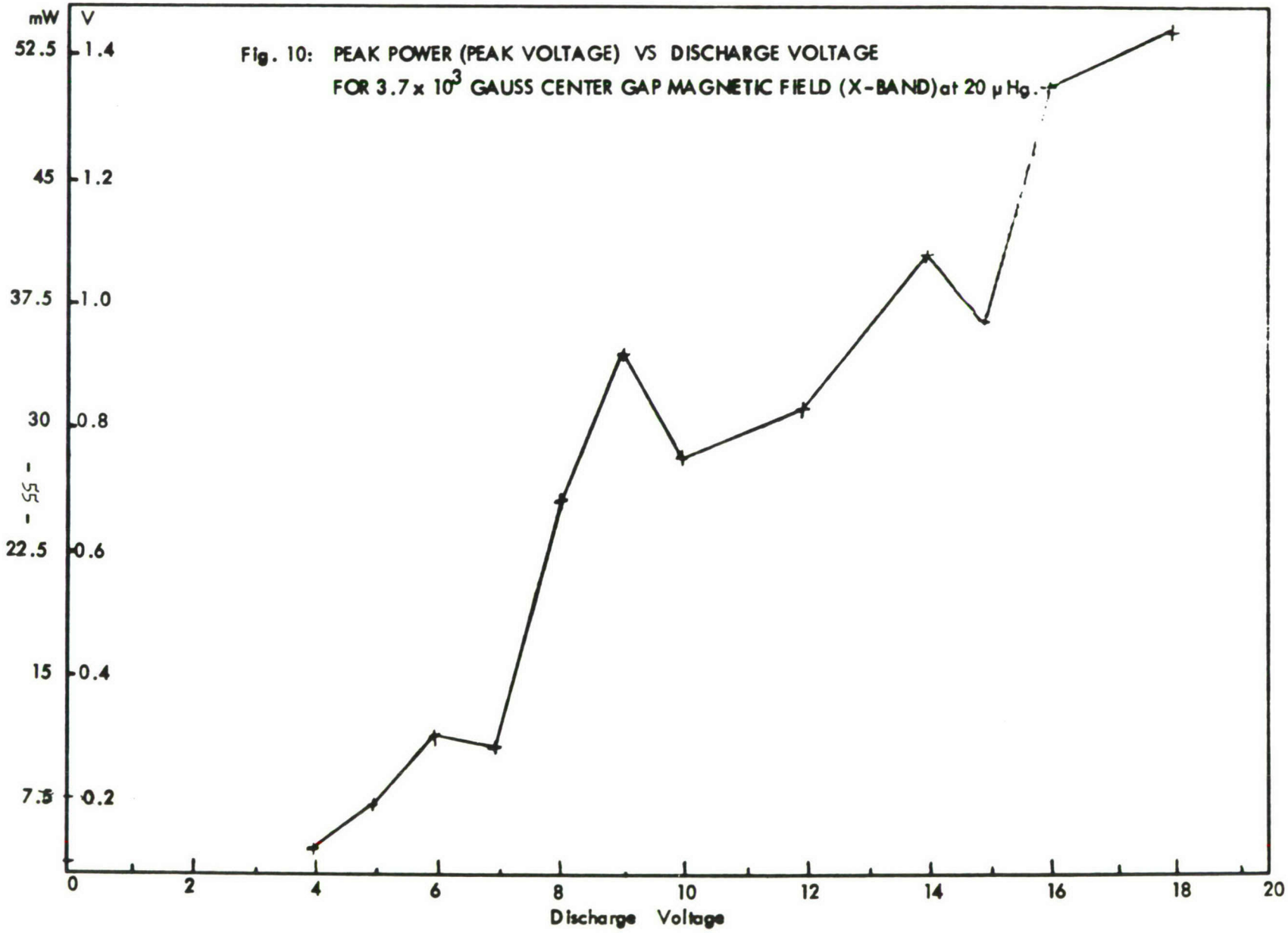

Fig. 10: PEAK POWER (PEAK VOLTAGE) VS DISCHARGE VOLTAGE FOR 3.7×10^3 GAUSS CENTER GAP MAGNETIC FIELD (X-BAND) at 20 μ Hg.

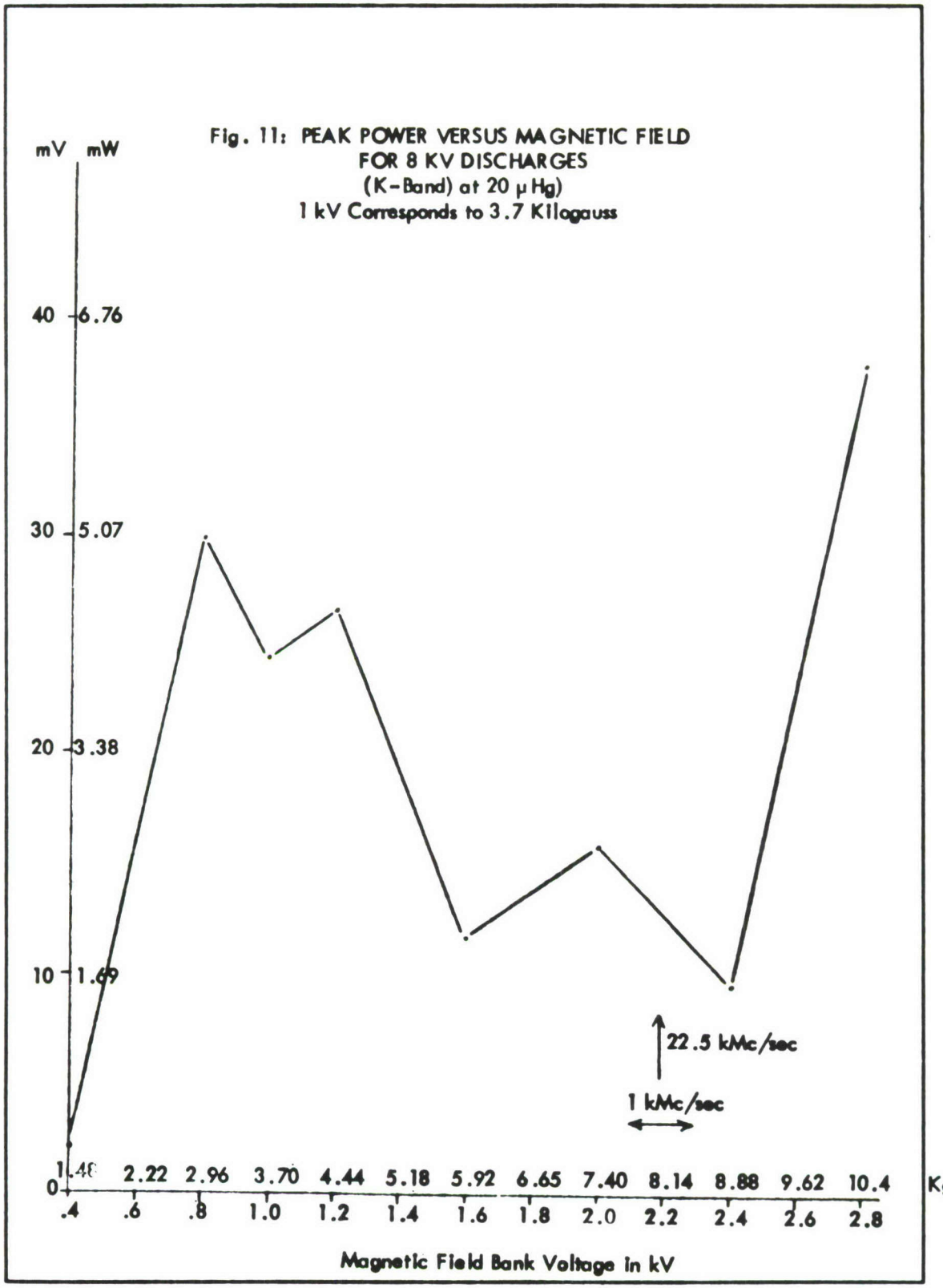

Fig. 11: PEAK POWER VERSUS MAGNETIC FIELD FOR 8 KV DISCHARGES (K-Band) at 20 μ Hg)
1 kV Corresponds to 3.7 Kilogauss

Fig. 12: PEAK POWER VS DISCHARGE VOLTAGE
FOR 3.7×10^3 GAUSS MAGNETIC FIELD

(K-Band) at 20 μ Hg.

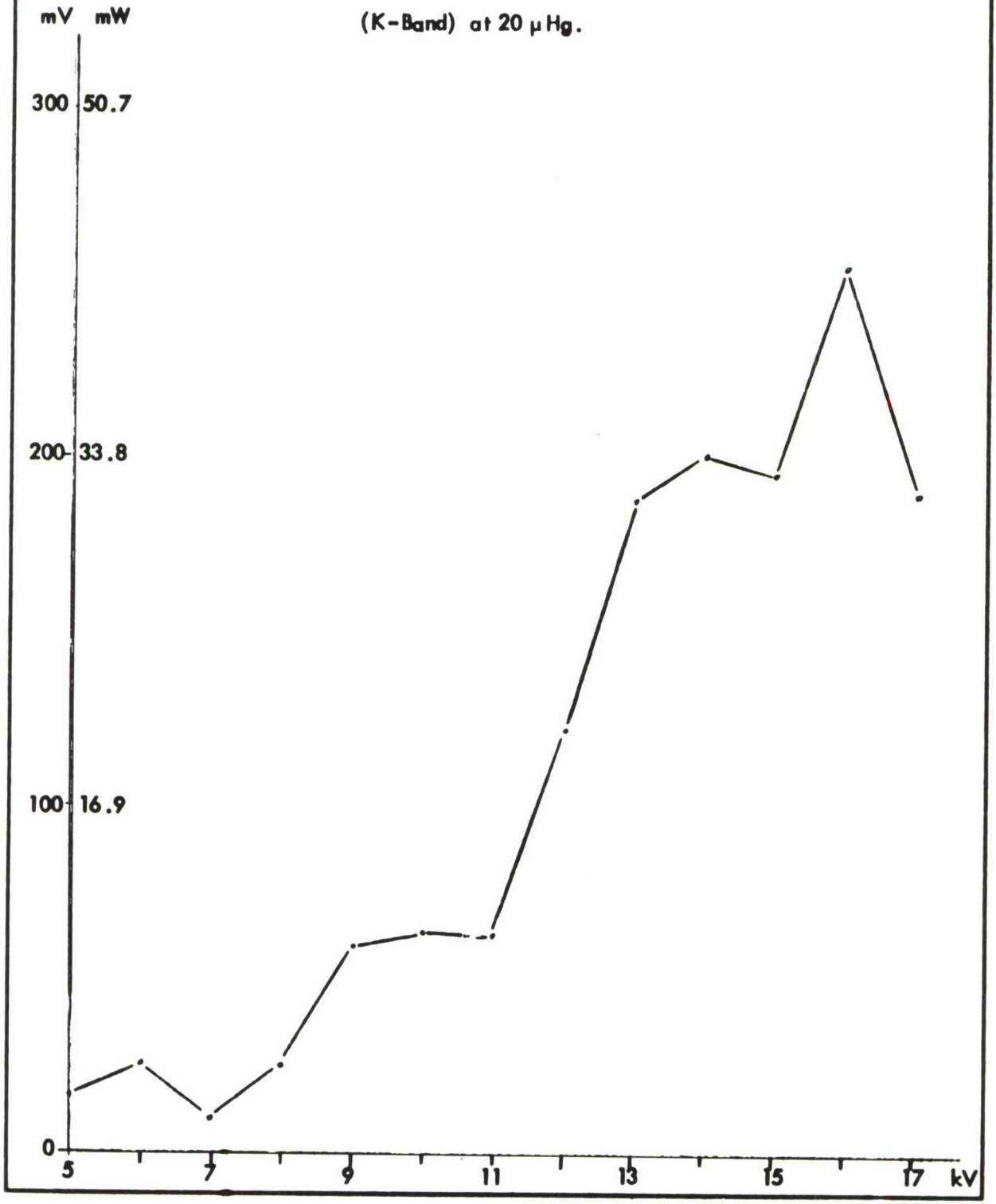

PIG Discharge Bank Voltage

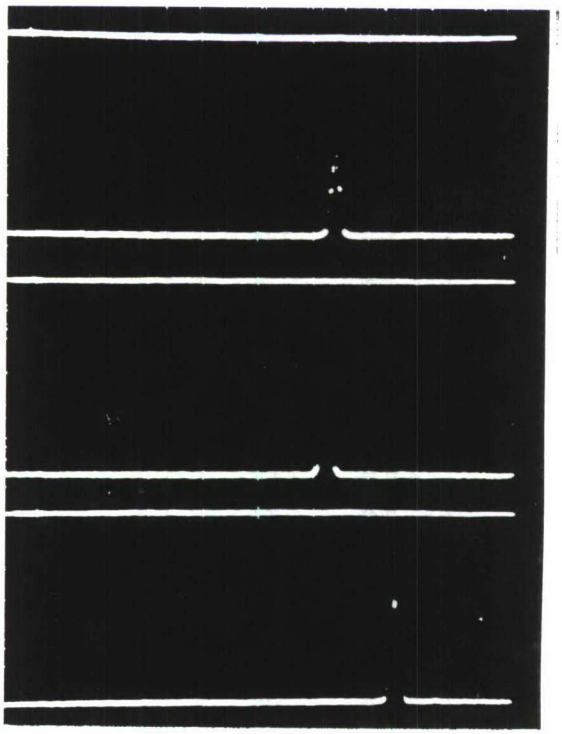

Fig. 13: TYPICAL OSCILLOGRAMS OF POWER DETECTED IN THE X-BAND BY 1N23B CRYSTAL.

The discharges took place in a 3.7 kilogauss magnetic field. 13a corresponds to a 12 kV discharge, and 13b and 13 c to 13 kV and 14 kV discharges, respectively.

Read time from right to left; positive direction is toward the top of the page. (Disregard upper trace of each pair.)

Voltage Sensitivity: 0.1 V/cm
Time Base: 0.5 μsec/cm

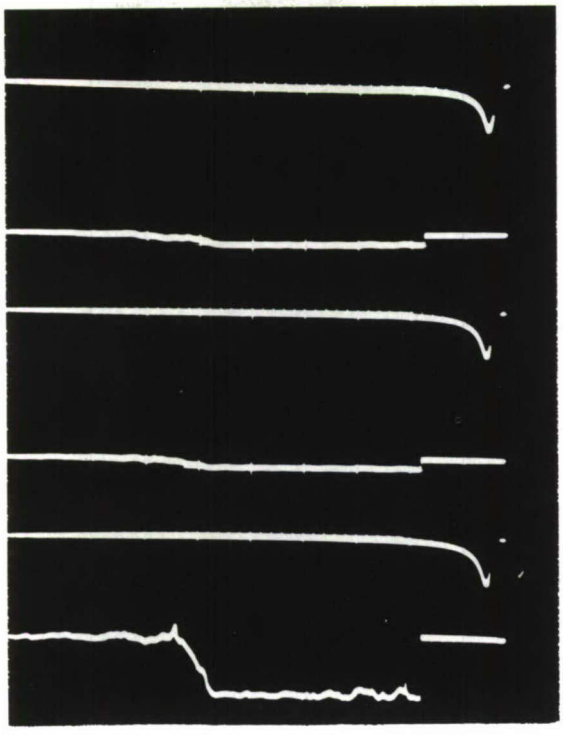

Fig. 14: TYPICAL OSCILLOGRAMS OF DETECTED POWER IN X-BAND MICROWAVE TRANSMISSION EXPERIMENT

A 9.35 kMc/sec cw signal was transmitted through the discharge and detected by a 1N23B crystal. The attenuation of the signal by the plasma is observed in 14a, b and c.

Read time from right to left; positive direction is toward the top of the page. (Disregard upper trace of each pair.)

Voltage Sensitivity:	13a, 13b - 50 mV/cm
	13c - 10 mV/cm
Time Base:	50 μsec/cm

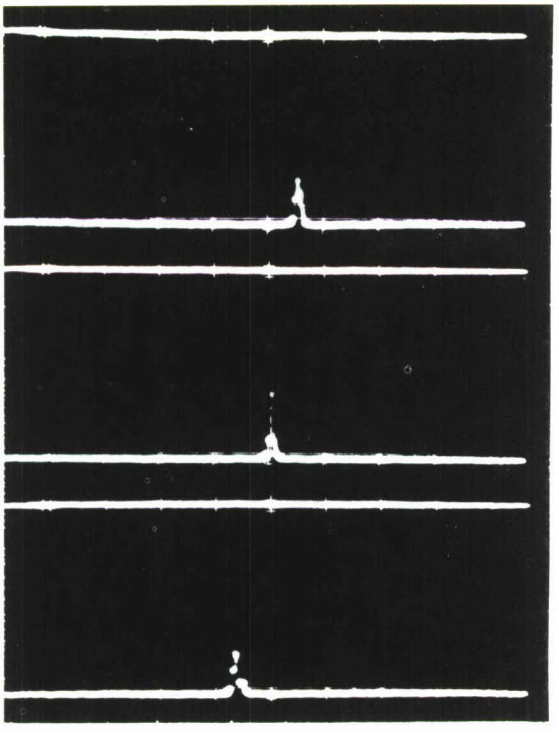

Fig. 15: TYPICAL OSCILLOGRAMS OF POWER DETECTED IN THE K-BAND BY A 1N26 CRYSTAL.

The discharge took place in a 3.7 kilogauss magnetic field. The detected signal is presumably due to 2nd harmonics of frequencies in the X-band. 13a is due to a 10 kV discharge, with 13b and 13c due to 8 kV and 9 kV discharges, respectively.

Voltage Sensitivity: 50 mV/cm
Time Base: 0.5 μsec/cm